ARTICLE

doi:10.1038/nature25154

Alcohol and endogenous aldehydes damage chromosomes and mutate stem cells

Juan I. Garaycoechea[1], Gerry P. Crossan[1], Frédéric Langevin[1], Lee Mulderrig[1], Sandra Louzada[2], Fentang Yang[2], Guillaume Guilbaud[1], Naomi Park[2], Sophie Roerink[2], Serena Nik-Zainal[2], Michael R. Stratton[2] & Ketan J. Patel[1,3]

Haematopoietic stem cells renew blood. Accumulation of DNA damage in these cells promotes their decline, while misrepair of this damage initiates malignancies. Here we describe the features and mutational landscape of DNA damage caused by acetaldehyde, an endogenous and alcohol-derived metabolite. This damage results in DNA double-stranded breaks that, despite stimulating recombination repair, also cause chromosome rearrangements. We combined transplantation of single haematopoietic stem cells with whole-genome sequencing to show that this damage occurs in stem cells, leading to deletions and rearrangements that are indicative of microhomology-mediated end-joining repair. Moreover, deletion of p53 completely rescues the survival of aldehyde-stressed and mutated haematopoietic stem cells, but does not change the pattern or the intensity of genome instability within individual stem cells. These findings characterize the mutation of the stem-cell genome by an alcohol-derived and endogenous source of DNA damage. Furthermore, we identify how the choice of DNA-repair pathway and a stringent p53 response limit the transmission of aldehyde-induced mutations in stem cells.

The consumption of alcohol contributes to global mortality and cancer development[1]. Most of the toxic effects of alcohol are probably caused by its oxidation product acetaldehyde, which is highly reactive towards DNA[2]. The enzyme aldehyde dehydrogenase 2 (ALDH2) prevents acetaldehyde accumulation by oxidizing it efficiently to acetate, but around 540 million people carry a polymorphism in *ALDH2* that encodes a dominant-negative variant of the enzyme[3]. Alcohol consumption in these individuals induces an aversive reaction and predisposes them to oesophageal cancer[4]. Nevertheless, ALDH2 deficiency is surprisingly well tolerated in humans. This could be because of the additional tier of protection provided by FANCD2, a DNA-crosslink-repair protein. In fact, genetic inactivation of *Aldh2* and *Fancd2* in mice leads to cancer and a profound haematopoietic phenotype[5,6]. In humans, deficiency in DNA-crosslink repair causes the inherited illness Fanconi anaemia, a devastating condition that leads to abnormal development, bone-marrow failure and cancer[7]. Acetaldehyde genotoxicity is likely to contribute to this phenotype, as Japanese children who are afflicted with Fanconi anaemia and carry the *ALDH2* polymorphism display earlier-onset bone marrow failure[8]. Together, these data suggest that endogenous aldehydes are a ubiquitous source of DNA damage that impairs blood production.

It is likely that some of this damage occurs in haematopoietic stem cells (HSCs), which are responsible for lifelong blood production. HSC attrition is a feature of ageing, and mutagenesis in the remaining HSCs promotes dysfunctional haematopoiesis and leukaemia. Moreover, both humans and mice that lack DNA repair factors are prone to HSC loss, and in some cases, bone marrow failure[9,10]. HSCs employ DNA repair and respond to damage in a distinct manner compared to later progenitors[11,12]. While these observations point to a fundamental role for DNA repair in HSCs, recent work has highlighted that the response to replication stress maintains HSC function and integrity[13]. However, there is a key gap in our knowledge regarding the identity of the endogenous factors that damage DNA and lead to replication stress. Here we show that alcohol-derived and endogenous aldehydes damage the genomes of haematopoietic cells, and we characterize the surveillance and repair mechanisms that counteract this. We also establish a method that allows us to determine the mutational landscape of individual HSCs, and in doing so, provide new insight into the p53 response in mutagenized stem cells.

Ethanol stimulates homologous recombination repair

Aldh2$^{-/-}$*Fancd2*$^{-/-}$ mice develop severe HSC attrition, causing spontaneous bone marrow failure, which can also be induced by exposing these mice to ethanol[5,6]. This genetic interaction suggests that in the absence of aldehyde catabolism (such as in *Aldh2*$^{-/-}$ mice), DNA repair is engaged to maintain blood homeostasis. To test this theory, we set out to monitor DNA repair activity *in vivo*. The Fanconi anaemia pathway repairs DNA crosslinks by using a replication-coupled excision mechanism that is completed by homologous recombination[14,15]. We therefore used a method to visualize sister-chromatid exchange (SCE) events in bone marrow cells of living mice; these represent recombination repair transactions coupled to replication (Fig. 1a). The number of SCE events is elevated 2.3-fold in *Aldh2*$^{-/-}$ mice, indicating that recombination repair is stimulated in response to endogenous aldehydes (Fig. 1b, c). Moreover, a single exposure to alcohol causes a fourfold increase in SCE events in *Aldh2*$^{-/-}$ mice (Fig. 1b, c, Extended Data Fig. 1a), suggesting that physiological acetaldehyde accumulation in blood cells is not sufficient to inactivate the homologous recombination repair factor BRCA2[16]. *Fancd2*$^{-/-}$ mice do not show a similar induction following exposure to ethanol; therefore, detoxification is the primary mechanism that prevents DNA damage by aldehydes and alcohol. Finally, the number of SCE events in *Aldh2*$^{-/-}$*Fancd2*$^{-/-}$ mice is indistinguishable from that in *Aldh2*$^{-/-}$ mice, showing that homologous recombination repair occurs despite inactivation of FANCD2 (Fig. 1c, Extended Data Fig. 1b).

The repair of aldehyde-induced DNA damage is therefore not limited to the Fanconi anaemia crosslink-repair pathway. As the recombination machinery is essential for mouse development, we used the isogenic chicken B-cell line DT40, which has been used to define the involvement of homologous recombination in crosslink repair[14].

[1]MRC Laboratory of Molecular Biology, Cambridge Biomedical Campus, Francis Crick Avenue, Cambridge CB2 0QH, UK. [2]Wellcome Trust Sanger Institute, Hinxton, Cambridge CB10 1SA, UK. [3]Department of Medicine, University of Cambridge, Addenbrooke's Hospital, Hills Rd, Cambridge CB2 0QQ, UK.

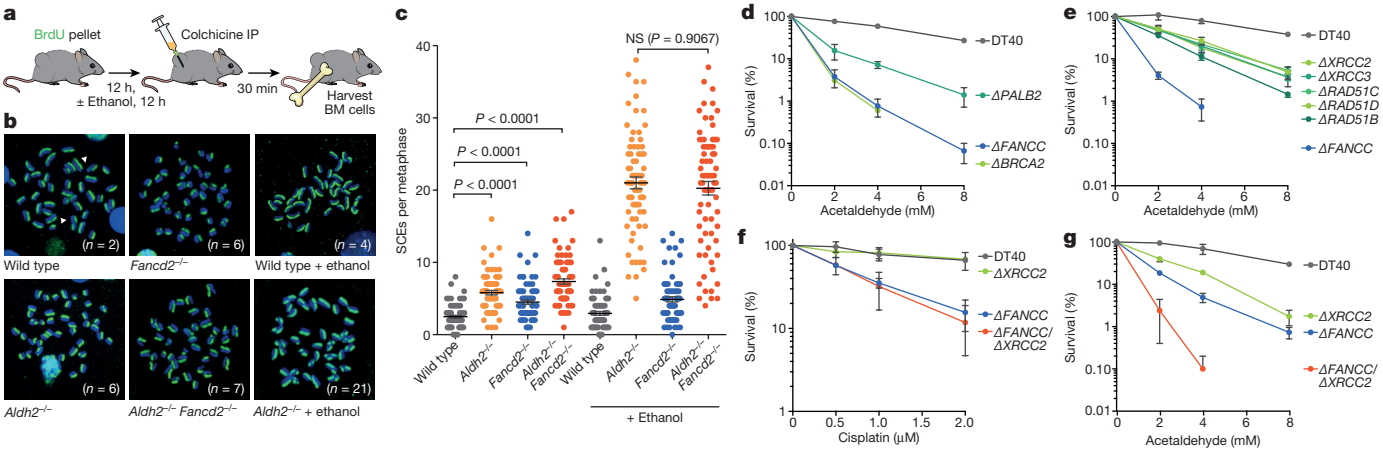

Figure 1 | Ethanol induces potent homologous recombination *in vivo*. **a**, Treatment of mice with BrdU for differential labelling of sister chromatids of bone marrow cells *in vivo*. Some mice were also treated with ethanol, a precursor of acetaldehyde. IP, intraperitoneal injection; BM, bone marrow. **b**, Representative images of bone-marrow metaphase spreads (*n*, number of SCEs per metaphase). **c**, Number of SCEs in the bone marrow of $Aldh2^{-/-}Fancd2^{-/-}$ and control mice (triplicate experiments, 25 metaphases per mouse, $n = 75$; *P* calculated by two-sided Mann–Whitney test; data shown as mean and s.e.m.). NS, not significant. **d**–**g**, Clonogenic survival of DT40 DNA-repair mutants (triplicate experiments; data shown as mean and s.e.m.).

DT40 cells carrying disruptions of key homologous recombination genes show hypersensitivity to acetaldehyde (Fig. 1d, e), in a similar way to cells lacking the Fanconi anaemia gene *FANCC*. To test the relationship between the Fanconi anaemia and homologous recombination pathways, we analysed the sensitivity of cells deficient in both *FANCC* and *XRCC2*. These cells showed the same sensitivity to cisplatin as the single knockout cells (Fig. 1f), but were much more sensitive to acetaldehyde (Fig. 1g), indicating that homologous recombination repair confers additional acetaldehyde resistance beyond that provided by Fanconi anaemia crosslink repair. In summary, detoxification provides the dominant protection mechanism against endogenous aldehydes; however, when aldehydes damage DNA, cells use both DNA-crosslink and homologous recombination repair.

FANCD2 prevents alcohol-induced genomic instability

The active DNA recombination in bone marrow cells indicates that even in the absence of FANCD2, there is an alternative repair response to both endogenous and ethanol-derived aldehydes. However, our previous work has shown that $Aldh2^{-/-}Fancd2^{-/-}$ mice lose the ability to maintain blood production[5,6]. To determine whether this is due to the accumulation of damaged DNA, we examined haematopoietic cells for evidence of broken chromosomes. One marker of genetic instability is the formation of micronuclei, which are formed from lagging or broken chromosomes. Micronuclei are easily quantified in normochromic erythrocytes (NCEs) *in vivo*, because they persist following enucleation (Fig. 2a, Extended Data Fig. 1c). There is a significant increase in the proportion of NCEs with micronuclei in

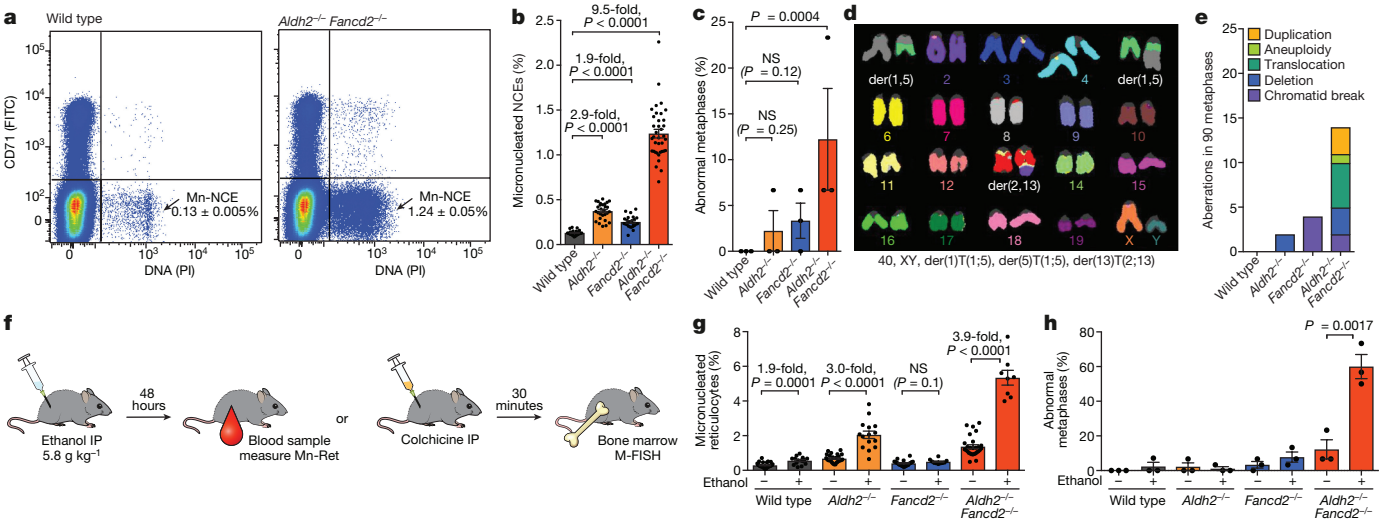

Figure 2 | Spontaneous and ethanol-induced genomic instability in $Aldh2^{-/-}Fancd2^{-/-}$ mice. **a**, Quantification of micronucleated normochromic erythrocytes (Mn-NCE, $CD71^{-}$ PI^{+}) by flow cytometry. **b**, Percentage of micronucleated normochromic erythrocytes (*P* calculated by two-sided Mann–Whitney test; data shown as mean and s.e.m.; $n = 28$, 28, 25 and 37 mice, left to right). **c**, Percentage of abnormal metaphases in bone marrow cells (*P* calculated by one-sided Fisher's exact test; data shown as mean and s.e.m.; three mice per genotype, 30 metaphases per mouse). **d**, A $Aldh2^{-/-}Fancd2^{-/-}$ metaphase, showing two translocations, see Extended Data Fig. 1f–i for the complete list of aberrations. **e**, Types of chromosomal aberrations (90 metaphases per genotype). **f**, Treatment of mice with ethanol to assess genomic instability with the micronucleus assay (**g**) or M-FISH karyotyping (**h**). **g**, Percentage of micronucleated reticulocytes (Mn-Ret, $CD71^{+}$ PI^{+}) after ethanol treatment. *P* calculated by two-sided Mann–Whitney test; data shown as mean and s.e.m.; $n = 29$, 15, 25, 15, 20, 10, 28 and 9 mice, left to right. **h**, Abnormal metaphases in bone marrow cells after ethanol treatment. *P* calculated by one-sided Fisher's exact test; data shown as mean and s.e.m.; 3 mice per genotype, 30 metaphases per mouse.

both *Aldh2*$^{-/-}$ (2.9-fold) and *Fancd2*$^{-/-}$ (1.9-fold) mice compared to wild-type controls, but the increase is much larger in *Aldh2*$^{-/-}$ *Fancd2*$^{-/-}$ mice (9.5-fold, Fig. 2b). These micronuclei could represent genomic instability during blood production. We therefore examined cells in metaphase obtained directly from the bone marrow of these mice with multiplex fluorescence *in situ* hybridization (M-FISH). More than 10% of *Aldh2*$^{-/-}$*Fancd2*$^{-/-}$ bone-marrow cells carried chromosomal aberrations, encompassing all classes of cytogenetic change (Fig. 2c–e). These aberrations are not clonal events, because each karyotype was unique (Extended Data Fig. 1).

Next, we investigated whether this chromosome damage was exacerbated by exposure to ethanol. As a control, we exposed wild-type or *Fancd2*$^{-/-}$ mice to mitomycin C (Extended Data Fig. 1d). The experimental scheme (outlined in Fig. 2f) shows how we determined the prevalence of micronuclei in reticulocytes and aberrant metaphases following exposure to ethanol. A single dose of ethanol caused a marked increase in the proportion of reticulocytes containing micronuclei in *Aldh2*$^{-/-}$ mice. Notably, this induction was comparable to that observed in wild-type mice following exposure to agents known to induce genome instability, such as ionizing irradiation or vincristine (Extended Data Fig. 1e). However, there was a stronger induction of micronucleus formation in *Aldh2*$^{-/-}$*Fancd2*$^{-/-}$ mice than in controls (Fig. 2g), which was accompanied by a striking increase in the number of abnormal metaphases, with almost 60% of metaphases having damaged chromosomes following ethanol exposure (Fig. 2h, Extended Data Fig. 1g–i). These mice rapidly lost the ability to produce blood and died from bone-marrow failure (Extended Data Fig. 2). These results show that, despite activation of homologous recombination, the Fanconi anaemia crosslink-repair pathway is essential for preventing chromosome breakage and loss of blood homeostasis in response to aldehydes.

Ku70 contributes to repair of aldehyde-induced DSBs

The presence of chromosome breaks and translocations suggests that aldehydes cause double-stranded breaks (DSBs), which could be processed by non-homologous end-joining (NHEJ) repair[17]. Previous studies in cell lines and nematodes have indicated that, in the absence of the Fanconi anaemia pathway, engagement of DSBs by NHEJ leads to further genomic instability[18,19]. Therefore, we investigated whether NHEJ and Fanconi anaemia repair are redundant in resolving endogenous DNA damage in HSCs, and whether there is a role for NHEJ in maintaining resistance to acetaldehyde.

To do this, we crossed mice deficient in the known Fanconi anaemia repair gene *Fanca* with mice lacking the key NHEJ factor Ku70 (encoded by *Xrcc6*, also known as *Ku70*). We failed to obtain *Fanca*$^{-/-}$*Ku70*$^{-/-}$ mice, indicating that there was a synthetic lethal interaction between Ku70-dependent NHEJ and Fanconi anaemia-crosslink repair (Supplementary Information Table 1). To bypass embryonic lethality, we generated blood-specific *Fanca* knockout mice (Extended Data Fig. 3) and crossed them with *Ku70*$^{+/-}$ mice to produce mice that had the double mutation in HSCs and the blood compartment (*Fanca*$^{fl/-}$*Ku70*$^{-/-}$ *Vav1*-iCre). These mice were viable, indicating that the embryonic lethality of *Fanca*$^{-/-}$*Ku70*$^{-/-}$ is not due to failed blood production (Supplementary Information Table 1). However, blood counts show that *Fanca*$^{fl/-}$*Ku70*$^{-/-}$ *Vav1*-iCre mice are anaemic (Fig. 3a) and have fewer HSCs compared to congenic controls (Fig. 3b–e). *Fanca*$^{fl/-}$*Ku70*$^{-/-}$ *Vav1*-iCre mice also display genomic instability, with increased frequency of micronuclei-containing NCEs (Fig. 3f). Finally, we tested whether Ku70 was required to maintain resistance of short-term (ST)-HSCs to aldehydes by exposing bone marrow cells to acetaldehyde *in vitro* before injecting them into lethally irradiated recipients. *Fanca*$^{fl/-}$*Ku70*$^{-/-}$ *Vav1*-iCre ST-HSCs were much more sensitive to acetaldehyde than either of the single mutant ST-HSCs (Fig. 3g). These results indicate that in the mouse haematopoietic system, in the absence of Fanconi anaemia repair, NHEJ is required to provide resistance to endogenous and acetaldehyde-induced DNA damage. This result contrasts with the reported negative impact of active NHEJ on the viability of Fanconi anaemia-deficient chicken DT40 cells and worms[18,19].

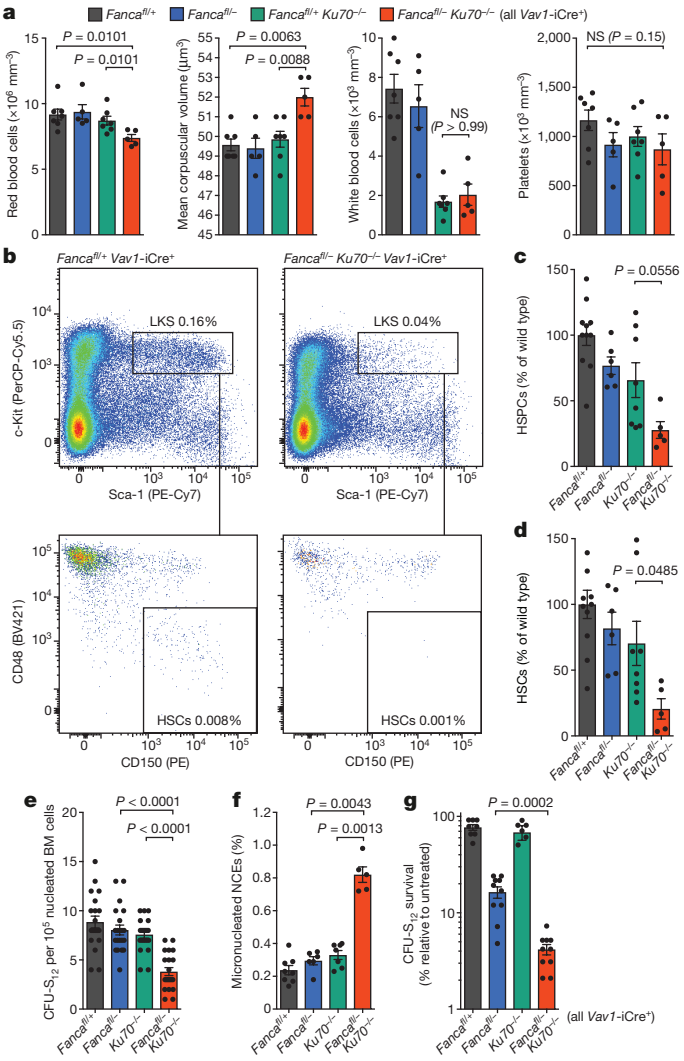

Figure 3 | NHEJ cooperates with the Fanconi anaemia pathway to maintain HSC integrity, genomic stability and cellular resistance to aldehydes. a, Blood parameters of 8- to 12-week old mice (*P* calculated by two-sided Mann–Whitney test; data shown as mean and s.e.m.; $n = 8$, 6, 7 and 5 mice, left to right). **b**, Representative flow cytometry plot of haematopoietic stem and progenitor cells (HSPCs) of *Fanca*$^{fl/-}$*Ku70*$^{-/-}$ *Vav1*-iCre mice and control. LKS, Lin$^-$Kit$^+$Sca-1$^+$. **c**, **d**, Quantification of HSPCs (Lin$^-$Kit$^+$Sca-1$^+$) and HSCs (Lin$^-$Kit$^+$Sca-1$^+$CD48$^-$CD150$^+$) by flow cytometry (*P* calculated by two-tailed Student's *t*-test; data shown as mean and s.e.m.; *n* as in **a**). **e**, Counts of colony-forming unit-spleen (CFU-S) colonies from the bone marrow of *Fanca*$^{fl/-}$*Ku70*$^{-/-}$ *Vav1*-iCre and control mice. Each point represents the number of CFU-S_{12} in a single recipient (*P* calculated by two-sided Mann–Whitney test; data shown as mean and s.e.m.; $n = 20$ mice). **f**, Frequency of Mn-NCE (*P* calculated by two-sided Mann–Whitney test; data shown as mean and s.e.m.; *n* as in **a**). **g**, Survival of CFU-S_{12} after treatment with 4 mM acetaldehyde for 4 h, relative to untreated samples (*P* calculated by two-sided Mann–Whitney test; data shown as mean and s.e.m.; $n = 10$ mice).

Aldehyde-damaged HSCs are functionally compromised

Our results so far indicate that endogenous aldehydes give rise to DSBs in the absence of Fanconi anaemia repair, which are engaged by homologous recombination and NHEJ, but ultimately rearrange chromosomes in bone marrow cells. A key question is whether endogenous DNA damage and subsequent mutations accumulate in the HSC

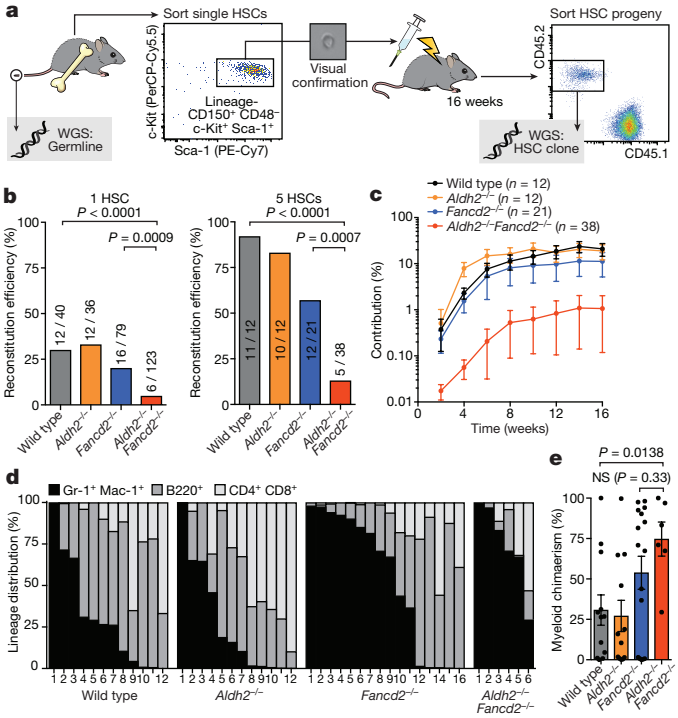

Figure 4 | Single HSC transplantation reveals that *Aldh2*$^{-/-}$*Fancd2*$^{-/-}$ HSCs are functionally compromised. a, Transplantation of single HSCs for the generation of HSC clones *in vivo*. The HSC progeny (CD45.2^{+}) were recovered after four months and analysed by whole-genome sequencing, alongside a germline reference. **b**, Percentage and number of irradiated recipients that were positive for reconstitution by one or five transplanted HSCs (*P* calculated by two-sided Fisher's exact test). **c**, Contribution to blood production over time by five transplanted HSCs (data shown as mean and s.e.m.). **d**, Lineage composition of single-HSC clones four months after transplant; columns represent individual recipients or clones. **e**, Proportion of myeloid (Gr-1^{+}Mac-1^{+}) HSC-derived white blood cells (*P* calculated by two-sided Mann–Whitney test; data shown as mean and s.e.m.; $n = 12$, 12, 16 and 6 HSC clones, left to right).

compartment. This is a critical question because there is evidence that HSCs differ in their DNA repair capacity and response compared to later progenitors[11]. Two obstacles had to be overcome in order to establish whether endogenous aldehydes mutate the genomes of these vital cells. First, the stochastic nature of DNA damage makes it unlikely that the same mutation will occur in multiple cells. Second, the scarcity of HSCs, especially in the case of *Aldh2*$^{-/-}$*Fancd2*$^{-/-}$ mice, precludes the use of most conventional techniques to assess DNA damage. We also wanted to ascertain whether mutations arise in functional stem cells, and therefore avoided whole-genome amplification or short-term *in vitro* expansion of cells isolated by flow cytometry. Instead, we decided to define HSCs functionally and exploit the ability of a single HSC to reconstitute long-term blood production following transplantation into a lethally irradiated mouse[20].

Our approach combines transplantation of single HSCs with whole-genome sequencing to obtain the mutational landscape of stem cells, while also allowing us to assess the functional capacity of mutant HSCs (Fig. 4a). We carried out transplants with one or five *Aldh2*$^{-/-}$*Fancd2*$^{-/-}$ HSCs (Fig. 4b). These stem cells rarely engrafted (with a frequency of 4.8%), contributed less to haematopoiesis and were myeloid-biased compared to controls (Fig. 4b–e). These results indicate that *Aldh2*$^{-/-}$*Fancd2*$^{-/-}$ HSCs are severely functionally compromised and share features with aged HSCs[21,22].

Mutational landscape of aldehyde-damaged stem cells

Our ultimate goal was to obtain clonal blood, which provided us with a physiological method to amplify stem-cell genomes. As outlined (Fig. 4a), four months after transplantation, we isolated the CD45.2^{+} HSC progeny and performed whole-genome sequencing at 20× coverage; tail DNA from the donor mouse served as the germline reference. This allowed us to detect heterozygous somatic changes, which are absent in the matched germline reference and represent mutations in the HSC. Genomes of *Aldh2*$^{-/-}$*Fancd2*$^{-/-}$ HSCs were mutated with increased prevalence of indels, rearrangements and translocations (Fig. 5a, Extended Data Fig. 4).

Although the number of single-base substitutions was significantly higher in *Aldh2*$^{-/-}$*Fancd2*$^{-/-}$ genomes (Fig. 5b), the total numbers were low and no changes were detected in the type of substitutions (Fig. 5c). We also found no difference in the frequency or pattern of point mutations in bone marrow cells of *Aldh2*$^{-/-}$*Fancd2*$^{-/-}$ mice using the SelectcII Big Blue *in vivo* reporter assay (Extended Data Fig. 5).

A limitation of our approach is that cells with the capacity to engraft may represent the least mutated HSCs. Nevertheless, we observed significant increases in the frequency of deletions, which were more prevalent (Fig. 5d, e) and larger (Fig. 5f) in *Aldh2*$^{-/-}$*Fancd2*$^{-/-}$ genomes. The mean variant allele frequency (VAF) for all filtered indels was 0.47, establishing that these changes are of clonal origin. By examining the flanking regions, we found that microhomology-mediated deletions are the main contributors to the mutations observed in *Aldh2*$^{-/-}$*Fancd2*$^{-/-}$ HSCs, indicative of end-joining repair of DSBs[23] (Fig. 5g, h). Additionally, the increase in the size of the deletions (Fig. 5f) suggests a role for alternative end-joining in the repair of some of these breaks, as alternative end-joining is characterized by increased resection in comparison to classical NHEJ[24]. Next, we analysed the location of indels across the genome, as recent work has suggested a role for the Fanconi anaemia pathway in preventing genomic instability at transcription–replication collisions[25,26]. However, we found no evidence of microhomology-mediated deletions being enriched at coding regions or transcribed genes (Fig. 5i, j), suggesting that DSB formation in *Aldh2*$^{-/-}$*Fancd2*$^{-/-}$ HSCs is stochastic.

The most striking change in *Aldh2*$^{-/-}$*Fancd2*$^{-/-}$ HSCs was the presence of rearrangements that were not detected in most controls. *Aldh2*$^{-/-}$*Fancd2*$^{-/-}$ stem cells contained on average two rearrangements per genome; in contrast, we observed only two large deletions among all ten control HSC genomes (Fig. 5k–l). In summary, these data

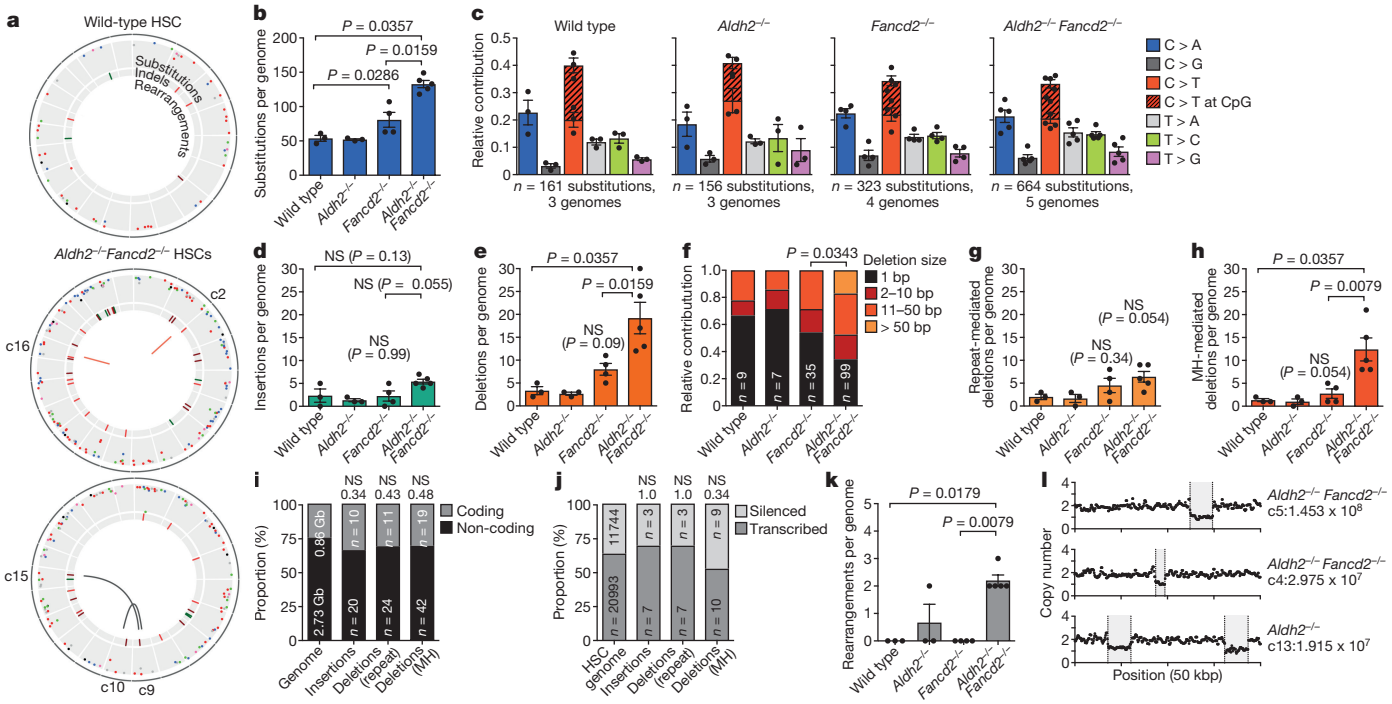

Figure 5 | Endogenous aldehydes mutate the HSC genome. a, Circos plots showing mutations in three HSCs. All HSCs are shown in Extended Data Fig. 4. **b**, **d**, **e**, **g**, **h**, **k**, Mutations of different classes per genome (*P* calculated by two-sided Mann–Whitney test; data shown as mean and s.e.m.; $n = 3$, 3, 4 and 5 HSC genomes, left to right). **b**, Number of substitutions. **c**, Point mutation classes in HSC genotypes. **d**, Number of insertions per genome. **e**, Number of deletions per genome. **f**, Distribution of the size of deletions (χ^2 test, *n* shows number of deletions). **g**, Number of repeat-mediated deletions per genome. **h**, Number of microhomology (MH)-mediated deletions per genome. **i**, **j**, Indels in *Aldh2*$^{-/-}$*Fancd2*$^{-/-}$ HSCs are randomly distributed: within or outside genes (**i**) (*P* calculated by hypergeometric distribution, *n* is number of indels), or between expressed or silenced genes (**j**) (*P* calculated by binomial distribution, *n* is number of indels). Numbers above columns, *P* values. **k**, Number of rearrangements per genome. **l**, Large copy-number losses in *Aldh2*$^{-/-}$*Fancd2*$^{-/-}$ and *Aldh2*$^{-/-}$ HSCs at the indicated locations.

provide the first whole-genome sequences obtained from single stem cells propagated *in vivo*. These stem cell genomes show that endogenous aldehydes induce a tapestry of inter-chromosomal changes that are mediated by mutagenic end-joining of DNA DSBs.

A p53 response removes aldehyde-damaged HSCs

Strikingly, most *Aldh2*$^{-/-}$*Fancd2*$^{-/-}$ HSCs failed to engraft (Fig. 4b). It is possible that HSCs that carry heavy DNA-damage burdens are eliminated, and selection pressure favours the survival of less damaged stem cells. It was therefore important to determine the mechanism of HSC loss in *Aldh2*$^{-/-}$*Fancd2*$^{-/-}$ mice, and if attenuated, it would be important to determine the mutagenic consequences. The p53 protein regulates the cellular response to DNA damage and, when activated, induces restorative processes or apoptosis. We found that *Aldh2*$^{-/-}$*Fancd2*$^{-/-}$ haematopoietic stem and progenitor cells (HSPCs) accumulated p53 and cleaved caspase-3, indicating that endogenous-aldehyde stress activates the p53 response (Extended Data Fig. 6a–c). Furthermore, we found that genetic ablation of p53 partially suppressed the acetaldehyde hypersensitivity of *Fancd2*-deficient splenic B cells and granulocyte/macrophage colony forming units (Extended Data Fig. 6d, e).

We therefore generated *Aldh2*$^{-/-}$*Fancd2*$^{-/-}$*Trp53*$^{-/-}$ triple-knockout mice. The severe HSC depletion of *Aldh2*$^{-/-}$*Fancd2*$^{-/-}$ mice was completely rescued in the triple knockouts (Fig. 6a, b). In addition, the triple-knockout stem cells were functional, as the mice showed a complete rescue in the frequency of ST-HSCs upon bone-marrow transplantation (Extended Data Fig. 6f). Moreover, p53 deficiency fully restored the blood cytopenias of untreated *Aldh2*$^{-/-}$*Fancd2*$^{-/-}$ mice and made these mice more resistant to alcohol exposure (Extended Data Fig. 7). Notably, *Trp53* deletion did not rescue the embryonic lethality of *Aldh2*$^{-/-}$*Fancd2*$^{-/-}$ embryos (in *Aldh2*$^{-/-}$ mothers), suggesting that a different checkpoint might mediate developmental failure (Supplementary Information Table 2).

We reasoned that the rescue of haematopoiesis in *Aldh2*$^{-/-}$*Fancd2*$^{-/-}$*Trp53*$^{-/-}$ mice must be occurring at the cost of genome integrity. Although the level of micronucleated NCEs in the blood of *Aldh2*$^{-/-}$*Fancd2*$^{-/-}$*Trp53*$^{-/-}$ mice appeared similar to that of *Aldh2*$^{-/-}$*Fancd2*$^{-/-}$ mice (Extended Data Fig. 8a), we noticed a significant ($P = 0.0034$) increase in chromosome rearrangements in *Aldh2*$^{-/-}$*Fancd2*$^{-/-}$*Trp53*$^{-/-}$ mice, as seen by M-FISH analysis of total bone marrow cells (Fig. 6c, Extended Data Fig. 8). However, neither of these analyses tell us whether genome stability is similarly compromised in *Aldh2*$^{-/-}$*Fancd2*$^{-/-}$*Trp53*$^{-/-}$ HSCs. We therefore performed transplantation of single HSCs combined with whole-genome sequencing, as described earlier, and observed that p53 deficiency partially rescued the engraftment defect of *Aldh2*$^{-/-}$*Fancd2*$^{-/-}$ HSCs (Fig. 6d). Surprisingly, the genomes of *Aldh2*$^{-/-}$*Fancd2*$^{-/-}$*Trp53*$^{-/-}$ stem cells did not carry a greater mutation burden compared to those of *Aldh2*$^{-/-}$*Fancd2*$^{-/-}$ HSCs (Fig. 6e, f). Indel and rearrangement calls were validated by targeted deep sequencing and PCR, respectively (Extended Data Figs 9, 10 and Methods). One plausible explanation for the lack of increased mutagenesis in *Aldh2*$^{-/-}$*Fancd2*$^{-/-}$*Trp53*$^{-/-}$ HSCs is the possibility that the very small number of HSCs in *Aldh2*$^{-/-}$*Fancd2*$^{-/-}$ mice might have undergone more replicative cycles, thereby accruing a larger number of mutations. To address this, we quantified the frequency of 'clock' mutations (C to T at CpG sites), but this analysis showed no significant difference between *Aldh2*$^{-/-}$*Fancd2*$^{-/-}$ and *Aldh2*$^{-/-}$*Fancd2*$^{-/-}$*Trp53*$^{-/-}$ HSCs (Fig. 6f). These results indicate that aldehyde-induced DNA damage induces p53 leading to HSC attrition, which is inconsistent with p53 being a negative regulator of Fanconi anaemia repair, as recently reported[27]. However, while *Trp53* deletion completely rescues HSC depletion, this does not occur at the expense of genome stability in blood stem cells.

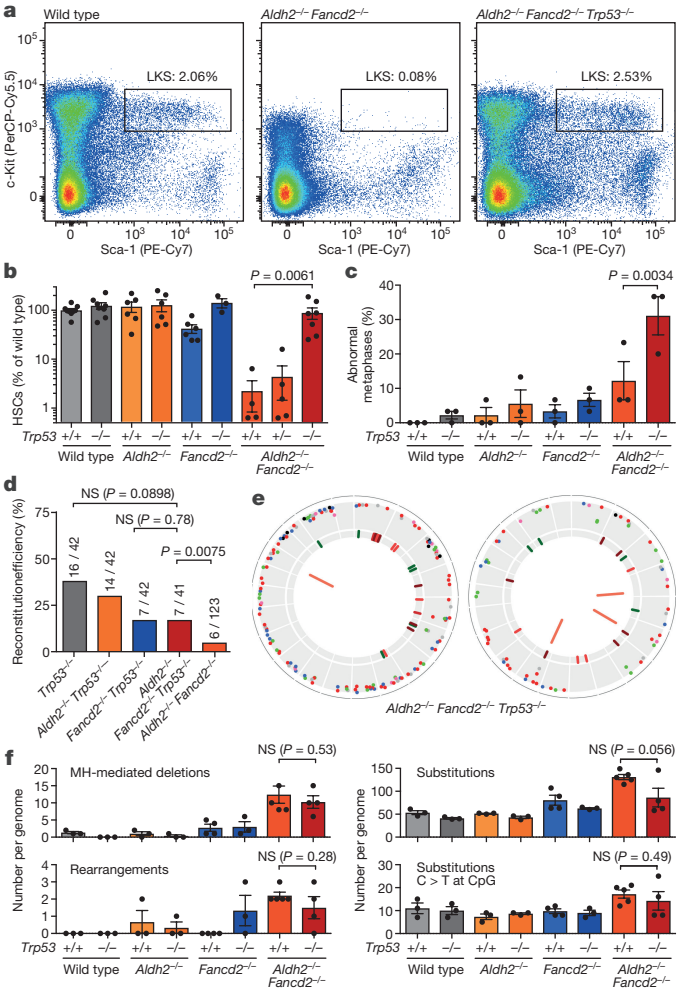

Figure 6 | A p53 response depletes aldehyde-damaged HSCs. **a**, Representative flow cytometry plot of HSPCs (LKS). **b**, Quantification of HSCs as determined by flow cytometry (*P* calculated by two-sided Mann–Whitney test; data shown as mean and s.e.m.; $n = 9, 8, 6, 6, 6, 3, 4, 5$ and 7 mice, left to right). **c**, Frequency of abnormal metaphases in bone marrow cells (*P* calculated by two-sided Fisher's exact test; data shown as mean and s.e.m.; 3 mice per genotype, 30 metaphases per mouse). See Extended Data Fig. 8b–d for a complete list of rearrangements. **d**, Proportion and number of irradiated recipients that were positive for reconstitution by transplantation of single HSCs (*P* calculated by two-sided Fisher's exact test). **e**, Mutations in two $Aldh2^{-/-}Fancd2^{-/-}Trp53^{-/-}$ HSCs. **f**, Number of microhomology-mediated deletions, rearrangements, substitutions and clock substitutions per genome (*P* calculated by two-sided Mann–Whitney test; data shown as mean and s.e.m.; $n = 3, 3, 3, 3, 4, 3, 5$ and 4 HSC genomes, left to right).

Discussion

These results outline the mechanisms by which the mouse haematopoietic system and, more specifically, blood stem cells respond to an endogenous and alcohol-derived source of DNA damage. Primary protection against acetaldehyde is provided by ALDH2-mediated detoxification and, when this is lost or saturated, acetaldehyde damages DNA. The Fanconi anaemia pathway is the principal mechanism to counteract this damage, but NHEJ and homologous recombination can also deal with these lesions. These results therefore illustrate that coordinated pathway choice is critical for maintaining genome stability upon aldehyde exposure. The Fanconi anaemia pathway prevents aldehyde lesions from degenerating into DSBs, the illegitimate repair of which leads to a characteristic pattern of mutagenesis in HSCs (Extended Data Fig. 11). Aldehydes are capable of forming a diverse range of DNA lesions—from base adducts to DNA–DNA or DNA–protein crosslinks. The known molecular function of the Fanconi anaemia pathway suggests that the most physiologically toxic lesion caused by aldehydes may be a DNA interstrand crosslink. However, if it is indeed an interstrand crosslink, then the factors involved in the translesion synthesis or homologous recombination processes are distinct from the previously described mechanism of interstrand-crosslink repair[6,14,15,28]. It will be important to resolve the nature of the lesion and the precise mechanics of its repair.

HSCs mutated by aldehydes are functionally compromised and display myeloid bias. The p53 response is critical in driving the loss in number and function of HSCs. Although *Trp53* deletion rescues HSC defects, this, paradoxically, does not result in further genomic instability at the single HSC level. It is important to emphasize, however, that the pool of HSCs is larger, and therefore there is still an overall increase in mutation. Nevertheless, our work implies that the relationship between p53, DNA repair and genome stability is more complex in stem cells than previously appreciated. The central role for ALDH2 in removing genotoxic aldehydes has implications for the more than 540 million people who are deficient in ALDH2 activity. Alcohol exposure in such individuals may cause DNA DSBs and chromosome rearrangements[3]. This large population may also be susceptible to alcohol-induced age-related blood disorders. More generally, this research provides a simple plausible explanation for the established epidemiological link between alcohol consumption and enhanced cancer risk[4,29].

Online Content Methods, along with any additional Extended Data display items and Source Data, are available in the online version of the paper; references unique to these sections appear only in the online paper.

Received 31 January; accepted 21 November 2017.
Published online 3 January 2018.

1. Roswall, N. & Weiderpass, E. Alcohol as a risk factor for cancer: existing evidence in a global perspective. *J. Prev. Med. Public Health* **48,** 1–9 (2015).
2. Wang, M. *et al.* Identification of DNA adducts of acetaldehyde. *Chem. Res. Toxicol.* **13,** 1149–1157 (2000).
3. Lai, C. L. *et al.* Dominance of the inactive Asian variant over activity and protein contents of mitochondrial aldehyde dehydrogenase 2 in human liver. *Alcohol. Clin. Exp. Res.* **38,** 44–50 (2014).
4. Yokoyama, A. & Omori, T. Genetic polymorphisms of alcohol and aldehyde dehydrogenases and risk for esophageal and head and neck cancers. *Jpn. J. Clin. Oncol.* **33,** 111–121 (2003).
5. Garaycoechea, J. I. *et al.* Genotoxic consequences of endogenous aldehydes on mouse haematopoietic stem cell function. *Nature* **489,** 571–575 (2012).
6. Langevin, F., Crossan, G. P., Rosado, I. V., Arends, M. J. & Patel, K. J. Fancd2 counteracts the toxic effects of naturally produced aldehydes in mice. *Nature* **475,** 53–58 (2011).
7. Garaycoechea, J. I. & Patel, K. J. Why does the bone marrow fail in Fanconi anemia? *Blood* **123,** 26–34 (2014).
8. Hira, A. *et al.* Variant ALDH2 is associated with accelerated progression of bone marrow failure in Japanese Fanconi anemia patients. *Blood* **122,** 3206–3209 (2013).
9. Nijnik, A. *et al.* DNA repair is limiting for haematopoietic stem cells during ageing. *Nature* **447,** 686–690 (2007).
10. Rossi, D. J. *et al.* Deficiencies in DNA damage repair limit the function of haematopoietic stem cells with age. *Nature* **447,** 725–729 (2007).
11. Milyavsky, M. *et al.* A distinctive DNA damage response in human hematopoietic stem cells reveals an apoptosis-independent role for p53 in self-renewal. *Cell Stem Cell* **7,** 186–197 (2010).
12. Mohrin, M. *et al.* Hematopoietic stem cell quiescence promotes error-prone DNA repair and mutagenesis. *Cell Stem Cell* **7,** 174–185 (2010).
13. Flach, J. *et al.* Replication stress is a potent driver of functional decline in ageing haematopoietic stem cells. *Nature* **512,** 198–202 (2014).
14. Niedzwiedz, W. *et al.* The Fanconi anaemia gene FANCC promotes homologous recombination and error-prone DNA repair. *Mol. Cell* **15,** 607–620 (2004).
15. Long, D. T., Räschle, M., Joukov, V. & Walter, J. C. Mechanism of RAD51-dependent DNA interstrand cross-link repair. *Science* **333,** 84–87 (2011).
16. Tan, S. L. W. *et al.* A class of environmental and endogenous toxins induces *BRCA2* haploinsufficiency and genome instability. *Cell* **169,** 1105–1118.e15 (2017).
17. Bunting, S. F. *et al.* 53BP1 inhibits homologous recombination in *Brca1*-deficient cells by blocking resection of DNA breaks. *Cell* **141,** 243–254 (2010).
18. Adamo, A. *et al.* Preventing nonhomologous end joining suppresses DNA repair defects of Fanconi anemia. *Mol. Cell* **39,** 25–35 (2010).
19. Pace, P. *et al.* Ku70 corrupts DNA repair in the absence of the Fanconi anemia pathway. *Science* **329,** 219–223 (2010).
20. Osawa, M., Hanada, K., Hamada, H. & Nakauchi, H. Long-term lymphohematopoietic reconstitution by a single CD34-low/negative hematopoietic stem cell. *Science* **273,** 242–245 (1996).

21. Dykstra, B., Olthof, S., Schreuder, J., Ritsema, M. & de Haan, G. Clonal analysis reveals multiple functional defects of aged murine hematopoietic stem cells. *J. Exp. Med.* **208,** 2691–2703 (2011).
22. Pang, W. W. *et al.* Human bone marrow hematopoietic stem cells are increased in frequency and myeloid-biased with age. *Proc. Natl Acad. Sci. USA* **108,** 20012–20017 (2011).
23. Ghezraoui, H. *et al.* Chromosomal translocations in human cells are generated by canonical nonhomologous end-joining. *Mol. Cell* **55,** 829–842 (2014).
24. Wyatt, D. W. *et al.* Essential roles for Polymerase θ-mediated end joining in the repair of chromosome breaks. *Mol. Cell* **63,** 662–673 (2016).
25. García-Rubio, M. L. *et al.* The Fanconi anemia pathway protects genome integrity from R-loops. *PLoS Genet.* **11,** e1005674 (2015).
26. Schwab, R. A. *et al.* The Fanconi anemia pathway maintains genome stability by coordinating replication and transcription. *Mol. Cell* **60,** 351–361 (2015).
27. Jaber, S., Toufektchan, E., Lejour, V., Bardot, B. & Toledo, F. p53 downregulates the Fanconi anaemia DNA repair pathway. *Nat. Commun.* **7,** 11091 (2016).
28. Oberbeck, N. *et al.* Maternal aldehyde elimination during pregnancy preserves the fetal genome. *Mol. Cell* **55,** 807–817 (2014).
29. Kawashima, N. *et al.* Aldehyde dehydrogenase-2 polymorphism contributes to the progression of bone marrow failure in children with idiopathic aplastic anaemia. *Br. J. Haematol.* **168,** 460–463 (2015).

Supplementary Information is available in the online version of the paper.

Acknowledgements We thank D. Kent for technical advice with single-HSC transplants; R. Berks, A. Middleton, J. Wiles, C. Knox, X. Gong, J. Roe, J. Willems, the ARES staff and Biomed for their help with mouse work; M. Daly, F. Zhang, V. Romashova and M. Balmont for help with flow cytometry; and J. Sale, C. Rada, M. Taylor, Y. L. Wu and members of the Patel laboratory for critical reading of the manuscript. The Human Research Tissue Bank (supported by the NIHR Cambridge Biomedical Research Centre) processed histology. K.J.P. is supported by the MRC and the Jeffrey Cheah Foundation. G.P.C. and L.M. were supported by CRUK. J.I.G. is supported by the Wellcome Trust and King's College, Cambridge.

Author Contributions J.I.G., G.P.C. and K.J.P. conceived the study and wrote the manuscript. J.I.G. conducted the majority of the experiments and analysed the data. G.P.C. assisted in the characterization of genomic instability in *Aldh2*$^{-/-}$*Fancd2*$^{-/-}$ mice and single HSC transplantation. F.L. analysed the survival of chicken DT40 cells, performed western blotting and assisted with the analysis of micronucleus samples. L.M. assisted with single cell transplantation and performed the BigBlue *in vivo* point-mutation analysis. S.L. and F.Y. performed the M-FISH karyotyping of mouse metaphases. N.P. performed validations of indels by targeted deep sequencing. G.G., S.R., S.N.-Z. and M.R.S. provided assistance with the analysis and interpretation of sequencing data.

Author Information Reprints and permissions information is available at www.nature.com/reprints. The authors declare no competing financial interests. Readers are welcome to comment on the online version of the paper. Publisher's note: Springer Nature remains neutral with regard to jurisdictional claims in published maps and institutional affiliations. Correspondence and requests for materials should be addressed to K.J.P. (kjp@mrc-lmb.cam.ac.uk).

METHODS

Mice. *Aldh2*$^{-/-}$*Fancd2*$^{-/-}$ mice were generated on a C57BL/6 × 129S4S6/Sv F_1 background. To this end, the previously reported *Fancd2* allele (*Fancd2*^{tm1Hou}; MGI ID: 2673422, a gift from M. Grompe) was back-crossed onto the C57BL/6Jo1a background for 10 generations and crossed with *Aldh2*$^{+/-}$ (C57BL/6N) mice to generate *Aldh2*$^{+/-}$*Fancd2*$^{+/-}$ mice on a pure C57BL/6 background. Likewise, the previously reported *Aldh2* allele (*Aldh2*$^{tm1a(EUCOMM)Wtsi}$; MGI ID: 4431566, EUCOMM[6]) was backcrossed from C57BL/6N onto 129S6/Sv for five generations and crossed with *Fancd2*$^{+/-}$ mice to generate *Aldh2*$^{+/-}$*Fancd2*$^{+/-}$ mice on a 129S4S6/Sv background. Finally, *Aldh2*$^{-/-}$*Fancd2*$^{-/-}$ and control mice were generated as F_1 hybrids from crosses between *Aldh2*$^{+/-}$*Fancd2*$^{+/-}$ females (129S4S6/Sv) and *Aldh2*$^{+/-}$*Fancd2*$^{+/-}$ males (C57BL/6).

To generate *Fanca*$^{-/-}$*Ku70*$^{-/-}$ mice on a pure C57BL/6 background, *Fanca*$^{+/-}$ mice (*Fanca*$^{tm1a(EUCOMM)Wtsi}$; MGI ID: 4434431, C57BL/6N, EUCOMM[5]) were crossed with *Ku70*$^{+/-}$ mice (*Xrcc6*^{tm1Fwa}, MGI ID: 2179954[30]), and the *Fanca*$^{+/-}$*Ku70*$^{+/-}$ progeny were then intercrossed to generate all possible genotypes. Pups from these crosses were genotyped at between two and three weeks old. For the generation of *Fanca*$^{fl/-}$*Ku70*$^{-/-}$*Vav1*-iCre^{+} tissue-specific double mutants (also on a pure C57BL/6 background), *Fanca*$^{+/-}$ mice were first crossed with FLP deletor mice[31] to produce the *Fanca* floxed allele (*Fanca*^{fl} or *Fanca*$^{tm1c(EUCOMM)Wtsi}$). Recombination of the Frt sites was verified by PCR (using the primers FL033, GCCTTTGCTGCTCTAATTCCATGT; FL040, TCAGCTCACTGAGACGCAACCTTTT ACACT; and En2A, GCTTCACTGAGTCTCTGGCATCTC), and reconstitution of FANCA expression was verified by western blotting spleen extracts of *Fanca*$^{fl/fl}$ mice (Extended Data Fig. 3). *Fanca*$^{+/fl}$ mice were then crossed with *Ku70*$^{+/-}$ mice to eventually produce *Fanca*$^{fl/fl}$*Ku70*$^{+/-}$ mice. Finally, these mice were crossed with *Fanca*$^{+/-}$*Ku70*$^{+/-}$ *Vav1*-iCre to generate *Fanca*$^{fl/-}$*Ku70*$^{-/-}$*Vav1*-iCre and control mice. The *Vav1*-iCre allele directs the expression of the iCre recombinase to HSCs and haematopoietic tissues[32], and in this case yields the *Fanca*-null allele (*Fanca*$^{\Delta}$ or *Fanca*$^{tm1d(EUCOMM)Wtsi}$). *Fanca*$^{\Delta/\Delta}$ mice phenocopy the *Fanca*$^{-/-}$ mice reported previously, as judged by FANCA expression, sterility and sensitivity to mitomycin C (Fig. 3, Extended Data Fig. 3).

Similarly to *Aldh2*$^{-/-}$*Fancd2*$^{-/-}$ F_1 mice, *Aldh2*$^{-/-}$*Fancd2*$^{-/-}$*Trp53*$^{-/-}$ mice were also generated in a C57BL/6 × 129S4S6/Sv F_1 background. In brief, the *Trp53* allele reported previously[33] was backcrossed onto 129S6/Sv or C57BL/6J for six generations. *Trp53*$^{+/-}$ mice were then intercrossed with *Aldh2*$^{-/-}$*Fancd2*$^{+/-}$ mice to establish parental (F_0) strains on both genetic backgrounds, which were finally crossed to obtain *Aldh2*$^{-/-}$*Fancd2*$^{-/-}$*Trp53*$^{-/-}$ and control F_1 mice.

For single HSC transplantation experiments, we used CD45.1 homozygous mice on a C57BL/6J × 129S6/Sv F_1 background as recipients. CD45.1 (or *Ptprc*^{a}) had been serially backcrossed from B6.SJL onto 129S6/Sv for six generations, with selection at each generation by serotyping with anti-CD45.1 (A20, FITC, BioLegend) and anti-CD45.2 antibodies (104, PE-Cy7, BioLegend).

For the *in vivo* point-mutation assay, mice carrying BigBlue λLIZ shuttle vector repeats (Stratagene) were crossed with *Aldh2*$^{-/-}$*Fancd2*$^{+/-}$ mice on a C57BL/6 × 129S4S6/Sv hybrid background. The resulting mice were intercrossed to obtain *Aldh2*$^{-/-}$*Fancd2*$^{-/-}$ BigBlue λLIZ and control mice.

For the analysis of Mendelian segregation of alleles, sample size was determined by power analysis using http://biomath.info/power/chsq1gp.htm. Sufficient mice to detect a 50% reduction in expected frequency were used, using power of 0.8 and alpha 0.05. No statistical methods were used to predetermine sample size in the other animal experiments. No randomization was employed. The investigators were blinded to the genotypes of mice throughout the study and data were acquired by relying purely on identification numbers.

All animals were maintained in specific pathogen-free conditions. In individual experiments all mice were matched for gender and age (8–12 weeks). All animal experiments undertaken in this study were done so with the approval of the UK Home Office.

Ethanol treatment. For acute ethanol exposure, *Aldh2*$^{-/-}$*Fancd2*$^{-/-}$ mice and appropriate controls were injected intraperitoneally with ethanol. The total dose of 5.8 g kg^{-1} was split into two injections separated by 4 h. Ethanol (96%, Sigma) was diluted to 28% v/v in saline, and administered twice at 13 ml kg^{-1}. Mice were exsanguinated 48 h after the second injection and peripheral blood was analysed with the micronucleus assay. Alternatively, mice were injected with colchicine for the preparation of metaphase spreads for M-FISH. For SCE analysis, mice were injected with colchicine 12 h after the second ethanol injection.

For chronic ethanol treatment of *Aldh2*$^{-/-}$*Fancd2*$^{-/-}$*Trp53*$^{-/-}$ and control mice, ethanol was administered in drinking water for ten days as reported previously[6]. For the first five days, the drinking water supply was replaced by a solution of 10:15:75 blackcurrant Ribena:ethanol:water, followed by a 10:20:80 solution for the last five days. A 50 μl blood sample was taken from tail veins before alcohol exposure, and by cardiac puncture at the end of the experiment, to measure full blood counts. Femurs were dissected for histological analysis and to determine bone marrow cellularity.

Preparation of mouse bone marrow for metaphase spreads. Treated or untreated young mice (8–12 weeks of age) were injected intraperitoneally with 100 μl of colchicine (0.5% w/v in water, Sigma). After 30 min the mice were culled by cervical dislocation, femurs were harvested and placed in ice-cold PBS. Bone marrow cells were flushed with 10 ml of pre-warmed hypotonic solution (75 mM KCl, 37 °C) through a 70-μm cell strainer and incubated for 15 min in a water bath at 37 °C. After the incubation, 1 ml of fixative (3:1 methanol:acetic acid) was added dropwise to the hypotonic buffer, and mixed by gentle inversion of the tube. The tubes were spun down for 10 min at 250 *g* and the supernatant was aspirated, leaving 50 μl and the cell pellet in the tube. The cells were resuspended by flicking the base of the tube very gently, 3 ml of fixative were added dropwise and the volume was made up to 10 ml by pipetting fixative down the side of the tube. The cells were incubated at room temperature for 30 min and stored at −20 °C until further use.

SCE assay for mouse bone marrow. The staining of metaphase spreads for the quantification of SCEs was adapted from published protocols[34,35]. A 50 mg BrdU slow-release pellet (Innovative Research of America) was surgically implanted subcutaneously into 8-to-12-week-old mice. Unchallenged mice were injected with colchicine 24 h later and metaphases were prepared after 30 min. Mice challenged with ethanol were injected intraperitoneally with ethanol 8 h and 12 h after implantation of the BrdU pellet. A total ethanol dose of 5.8 g kg^{-1} was split between these two doses as described previously. Metaphases were prepared as outlined above. Cells were then dropped from a height of 30 cm onto chilled, humidified slides. The slides were then dried for 1 h at 62 °C in a hybridization oven. Cells were washed in 2× SSC for 5 min at room temperature. Cells were stained for 15 min at room temperature with 1 μg ml^{-1} Hoechst 33258 pentahydrate (H3569, Molecular Probes) in 2× SSC. The slides were then transferred to a Petri dish with 2× SSC and exposed to UV irradiation for 30 min in a Stratalinker Crosslinker (Stratagene). The slides were then dehydrated by passing them through an ethanol series (70%, 96% and 100%) and placed in PBS for 5 min at room temperature. The DNA was denatured by exposure to 0.07 N NaOH for 2 min at room temperature. The slides were then washed three times in PBS for 5 min. The slides were then blocked in PBS, 1% BSA, 0.5% Tween-20 for 1 h at room temperature and stained overnight with a FITC-conjugated mouse anti-BrdU antibody (Clone B44, BD Biosciences) diluted 1:1 in PBS, 3% BSA, 0.5% Tween-20 at room temperature. The slides were then washed three times with PBS, 1% BSA, 0.5% Tween-20 for 5 min at room temperature and stained with goat anti-mouse Alexa Fluor-488 secondary antibody (A-11001, Life Technologies) diluted 1:500 in PBS, 1% BSA, 0.5% Tween-20 for 6 h at room temperature. The slides were then washed three times in PBS, 1% BSA, 0.5% Tween-20 for 15 min and stained with Hoechst 33342 trihydrochloride (H3570, Molecular Probes) diluted 1:2000 in PBS for 15 min at room temperature. The slides were then washed three times in PBS for 10 min on each occasion, washed once in water for 5 min, mounted with ProLong Gold Antifade Mountant (P36930, Molecular Probes) and coverslips were lowered onto the slides. Thirty metaphases were captured per sample using a Zeiss LSM 780 confocal microscope (Zeiss). The number of sister-chromatid exchanges per metaphase was then counted blind.

M-FISH karyotyping. For M-FISH, chromosome-specific DNA libraries were generated from flow-sorted chromosomes provided by the Flow Cytometry Core Facility of the Wellcome Trust Sanger Institute, using the GenomePlex Complete whole-genome amplification kit (Sigma–Aldrich). A mouse 21-colour painting probe was prepared following the pooling strategy[36]. Five mouse-chromosome pools were each labelled with ATTO 425-, ATTO 488-, Cy3-, Cy5- and Texas Red-dUTPs (Jena Bioscience), respectively, using the GenomePlex WGA reamplification kit (Sigma–Aldrich) and a dNTP mixture as described previously[37]. The labelled products were pooled and sonicated to achieve a size range of 200–1,000 bp, optimal for use in chromosome painting. The sonicated DNA was ethanol-precipitated together with mouse Cot-1 DNA (Thermo Fisher Scientific), and resuspended in a hybridization buffer (50% formamide, 2× SSC, 10% dextran sulfate, 0.5 M phosphate buffer, 1× Denhardt's solution, pH 7.4). Bone marrow cells suspended in fixative as described above (3:1 methanol:acetic acid) were dropped onto precleaned microscope slides, followed by fixation in acetone (Sigma–Aldrich) for 10 min and dehydration through an ethanol series (70%, 90% and 100%). Metaphase spreads on slides were denatured by immersion in an alkaline denaturation solution (0.5 M NaOH, 1.0 M NaCl) for 2 min, followed by rinsing in 1 M Tris-HCl (pH 7.4) solution for 3 min, 1× PBS for 3 min and dehydration through a 70%, 90% and 100% ethanol series. The M-FISH probes were denatured at 65 °C for 10 min before being applied onto the denatured slides. The hybridization area was sealed with a 22 mm × 22 mm coverslip and rubber cement. Hybridization was carried out in a 37 °C incubator for approximately 44–48 h. The post-hybridization washes included a 5-min stringent wash in 0.5× SSC at 75 °C, followed by a 5 min rinse in 2× SSC containing 0.05% Tween-20 (VWR) and a

2 min rinse in 1× PBS, both at room temperature. Finally, slides were mounted with SlowFade Gold mounting solution containing DAPI (Thermo Fisher Scientific). M-FISH images were visualized on a Zeiss AxioImager D1 fluorescent microscope equipped with narrow band-pass filters for DAPI, DEAC, FITC, Cy3, Texas Red and Cy5 fluorescence and an ORCA-EA CCD camera (Hamamatsu). M-FISH digital images were captured using the SmartCapture software (Digital Scientific UK), and processed using the SmartType Karyotyper software (Digital Scientific UK). Thirty metaphases for each sample were karyotyped by M-FISH.

DT40 clonogenic survival. DT40 cells were grown in RPMI Medium 1640 (Life Technologies, 61870), supplemented with 7% fetal bovine serum (FBS, Life Techonologies, 10270), 3% chicken serum (Life Technologies, 16110), 50 μM β-mercaptoethanol and penicillin/streptomycin, at 37 °C in a 5% CO_2 incubator. Sensitivity assays were performed as previously described[6]. In brief, 10^5 cells were incubated with drug-containing medium in a sealed FACS tube at 37 °C for 2 h (acetaldehyde) or 1 h (mitomycin C or cisplatin). Dilutions were plated in 6-well plates containing semi-solid medium (4000 cP methyl cellulose (M0512 Sigma), DMEM/F-12 powder (Life Technologies, 32500-043), 7% FBS, 3% chicken serum, 50 μM β-mercaptoethanol and penicillin/streptomycin). Plates were incubated for 7–10 days, after which time colonies were counted manually. Survival is plotted as a percentage relative to untreated cells. Each data point represents the mean of three independent experiments each carried out in quadruplicate.

Sensitivity assays of primary mouse B cells. These assays were performed as described previously[5]. Lymphocytes purified from the spleen using Lympholyte M (Cederlane) were stimulated with lipopolysaccharide (L4391, Sigma) at a final concentration of 40 μg ml^{-1}. Cells (4×10^5) were then plated with acetaldehyde in one well of a 24-well plate. After seven days, viable cells were counted using trypan blue exclusion from 100 images on a Vi-Cell XR cell viability counter (Beckman Coulter). Each data point represents the mean of three independent experiments each carried out in quadruplicate.

Survival assays of colony-forming units (CFU). Bone marrow cells were isolated using IMDM medium, and single cell suspensions were obtained by passing the bone marrow through a 70-μm cell strainer (Falcon). Nucleated cells were counted by diluting cells tenfold in a 3% solution of acetic acid with methylene blue (Stem Cell Technologies) using a Vi-Cell XR cell viability counter (Beckman Coulter). Cells were resuspended to make up 1.5 ml of IMDM containing 30×10^6 cells and 250 μl of each suspension was mixed with 250 μl of IMDM containing 2× acetaldehyde to give final concentrations of 0, 1, 2, 4 and 8 mM acetaldehyde. The cells were incubated at 37 °C for 4 h in sealed tubes, after which two tenfold serial dilutions were made. 400 μl of cells were then added to 4 ml of MethoCult M3534 (StemCell Technologies), and the total volume of each dilution was plated in two wells of a six-well plate each containing 10^6, 10^5 and 10^4 cells, respectively. After seven days of culture at 37 °C with 5% CO_2, the colonies were counted and the relative survival was plotted. Each data point represents the average of experimental duplicates carried out on three mice of each genotype.

Flow cytometry. The micronucleus assay was performed essentially as described previously[38]. Treated or untreated mice (8–12 weeks of age) were bled and 62 μl blood was mixed with 338 μl PBS supplemented with 1,000 U ml^{-1} of heparin (Calbiochem). 360 μl of blood suspension was then added to 3.6 ml of methanol at −80 °C and stored at −80°C for at least 12 h. 1 ml of fixed blood cells was then washed with 6 ml of bicarbonate buffer (0.9% NaCl, 5.3 mM $NaHCO_3$). The cells were resuspended in 150 μl of bicarbonate buffer and 20 μl of this suspension was used for subsequent staining. 72 μl of bicarbonate buffer, 1 μl of FITC-conjugated CD71 antibody (GenTex, clone R17217.1.4) and 7 μl RNase A (Sigma) were premixed and added to 20 μl of each cell suspension. The cells were stained at 4 °C for 45 min, followed by addition of 1 ml bicarbonate buffer and centrifugation. Finally, cell pellets were resuspended in 500 μl bicarbonate buffer supplemented with 5 μg ml^{-1} propidium iodide (Sigma). The samples were analysed immediately on an LSRII FACS analyser (BD) and the data analysed with FlowJo v10.0.7.

For HSC quantification, bone marrow cells were isolated from tibiae and femurs with staining buffer (PBS supplemented with 2.5% FCS) and strained through 70-μm meshes. Red cells were lysed by resuspending the cells in 10 ml red cell lysis buffer (MACS Miltenyi Biotec) for 10 min at room temperature. After centrifugation, the cell pellet was resuspended in staining buffer and nucleated cells were counted with 3% acetic acid (StemCell Technologies) on a Vi-Cell XR cell viability counter (Beckman Coulter). Bone marrow cells (10×10^6 cells) were resuspended in 200 μl of staining buffer containing the following antibody solution: FITC-conjugated lineage cocktail with antibodies against CD4 (clone H129.19, BD Pharmingen), CD3e (clone 145-2C11, eBioscience), Ly-6G/Gr-1 (clone RB6-8C5, eBioscience), CD11b/Mac-1 (clone M1/70, BD Pharmingen), CD45R/B220 (clone RA3-6B2, BD Pharmingen), Fcε R1α (clone MAR-1, eBioscience), CD8a (clone 53-6.7, BD Pharmingen), CD11c (clone N418, eBioscience), TER-119 (clone Ter119, BD Pharmingen) and CD41 (FITC, clone MWReg30, BD Pharmigen); c-Kit (PerCP-Cy5.5, clone 2B8, eBioscience), Sca-1 (PE-Cy7, clone D7, eBioscience), CD150 (PE, clone TC15-12F12.2, BioLegend) and CD48 (biotin, clone HM48-1, BioLegend). The samples were incubated for 15 min at 4 °C and washed with 2 ml buffer. The cell pellets were resuspended in 200 μl staining buffer containing streptavidin-BV421 and incubated for another 15 min at 4 °C. Finally, cells were washed, resuspended in 500 μl staining buffer, data were acquired on a Fortessa FACS analyser (Becton Dickinson) and analysed with FlowJo v10.0.7. LKS cells were defined as lineage$^-$ CD41$^-$Sca-1$^+$ Kit$^+$ and HSCs were defined as LKS CD48$^-$ CD150$^+$.

To assess engraftment of single HSCs into irradiated recipients, 50 μl of blood was obtained from the tail vein of recipient mice every two weeks. RBCs were lysed by the addition of 1 ml of ammonium chloride lysis buffer (155 mM NH_4Cl, 10 mM $KHCO_3$, 0.1 mM Na_2EDTA, pH 7.2) and incubated for 10 min at room temperature. After centrifugation, the cell pellets were resuspended in 100 μl of staining buffer containing antibodies against: CD4 (FITC, clone H129.19, BD Pharmingen), CD8a (FITC, clone 53-6.7, BD Pharmingen), CD45R/B220 (PerCP-Cy5.5, clone RA3-6B2, BioLegend), CD11b/Mac-1 (PE, clone M1/70, BD Pharmingen), Ly-6G/Gr-1 (PE, clone 1A8, BD Pharmingen), TER-119 (PE-Cy7, clone TER-119, BioLegend), CD45.1 (BV421, clone A20, BioLegend) and CD45.2 (APC, clone 104, BioLegend). After incubation, cells were washed with 3 ml of staining buffer before being resuspended in 250 μl of the same buffer. Samples were run on the Fortessa analyser (BD) with the HTS module and the multilineage chimaerism was calculated using FlowJo v10.0.7. TER-119 was used to exclude RBC debris and chimaerism was calculated for each of the WBC lineages (CD45$^+$ total WBCs, B220$^+$ B cells, CD4$^+$CD8$^+$ T cells and Gr-1$^+$ Mac-1$^+$ myeloid cells) as the proportion of cells derived from the single HSC (CD45.2$^+$) over the total number of CD45$^+$ cells, which includes cells derived from the recipient or carrier cells (CD45.1$^+$).

For intracellular staining of p53 and cleaved caspase-3, total bone marrow cells were stained with the lineage-depletion kit (130-090-858, MACS Miltenyi Biotec) following the manufacturer's instructions and passed through LS magnetic columns. Lineage-depleted cells were spun down for 5 min at 1,200 r.p.m. and the pellets were resuspended in 200 μl MACS buffer with the antibodies described above for HSC quantification. In parallel, 3×10^6 total bone marrow cells were stained with antibodies against committed lineages: CD45R/B220 (PE, clone RA3-6B2, BD Pharmingen) and IgM (FITC, clone II/41, BD Pharmingen) for B cell progenitors; TER-119 (FITC, clone TER-119, BD Pharmingen) and CD71 (PE, clone C2, BD Pharmingen) for erythroid maturation; and CD11b/Mac-1 (PE, clone M1/70, BD Pharmingen) and Ly-6G/Gr-1 (FITC, clone 1A8, eBioscience) for monocyte/granulocyte progenitors. After antibody staining, cells were washed, then fixed and permeabilized with BD Cytofix/Cytoperm solution (554722, BD Pharmingen) following the manufacturer's instructions. Finally, cells were stained with either anti-p53 (AlexaFluor647, clone 1C12, Cell Signalling) or anti-cleaved-caspase-3 (AlexaFluor647, clone D3E9, Cell Signalling) antibodies.

Gating strategies are described in Supplementary Fig. 2.

Blood counts. Total blood was collected in K3EDTA MiniCollect tubes (Greiner bio-one) and analysed on a VetABC analyser (Horiba).

Western blot. The FANCA antibody (Cell Signalling, D1L2Z) was used at 1:1000 in 5% w/v BSA, 1× TBS, 0.1% Tween-20 at 4 °C with gentle shaking, overnight. The β-actin antibody (Abcam, 8227) was used at 1:3,000 in the same conditions. Swine anti-rabbit immunoglobulins HRP (Dako) was used as secondary antibody at 1:2,000 for 1 h at room temperature.

Histological analysis. Tissue samples were fixed in 10% neutral-buffered formalin for at least 24 h. The femur samples were then decalcified and embedded in paraffin, and 4 μm sections were cut before staining with haematoxylin and eosin using standard methods.

***In vivo* point mutation assay.** The λ select-cII (BigBlue) mutagenesis assay was performed following the manufacturer's instructions. This assay allows the detection of point mutations *in vivo* and is based on the ability of coliphage λ to multiply either through the lytic or lysogeneic cycles in *Escherichia coli*.

In brief, the RecoverEase DNA-isolation kit (Stratagene) was used to extract genomic DNA from the bone marrow of 8-to-12-week old *Aldh2*$^{-/-}$*Fancd2*$^{-/-}$ and control mice that carry Big Blue λLIZ repeats. The shuttle vector that was recovered from mouse genomic DNA was packaged into phage with the Transpack packaging extract (Stratagene), which was then used to infect *E. coli* G1250 (Stratagene).

To assess the frequency of mutations within the *cII* gene, infected *E. coli* were diluted in TB1 top agar, spread on ten 100-mm TB1-agar plates and incubated at 24 °C for 48 h. The plaques were enumerated, picked and replated to confirm that they were lytic. This provided the number of mutated phage within the sample. To determine the total number of phage undergoing the lysogenic cycle and the mutation frequency, 10-and-50-fold dilutions of the stock of infected *E. coli* in TB1 top agar were spread on two 100-mm TB1-agar plates and incubated at 37 °C for 24 h. Incubation at 37 °C switches all phage to the lytic cycle, and therefore allows the total number of replication-competent phage to be assessed. The mutation

frequency was then calculated as the number of *cII*-mutated plaques (24 °C)/total number of plaques (37 °C).

As a positive control for the *in vivo* λ select-*cII* mutagenesis assay, mice were exposed to 150 mg kg^{-1} N-ethyl-N-nitrosourea (ENU, Sigma) in a single intraperitoneal injection on one occasion. Mice were allowed to recover and were euthanized 3 weeks later.

CFU-S_{12} assays. CFU-S_{12} assays were performed as described previously[5], except that CFU-S colonies were counted after 12 days. In brief, to assess the frequency of CFU-S in mutant mice, total bone marrow was flushed from the femora and tibiae of mutant mice and appropriate controls. Nucleated cells were enumerated using a solution of 3% acetic acid and methylene blue and injected intravenously into 20 recipient mice that had been lethally irradiated. After 12 days the spleens were fixed in Bouin's solution (Sigma), and the number of colonies were counted and expressed relative to the number of total bone marrow cells injected.

To assess the survival of CFU-S_{12} after exposure to acetaldehyde, we treated total bone marrow cells with 4 mM acetaldehyde for 4 h *in vitro* before injecting them into lethally irradiated recipient mice. After 12 days, the number of CFU-S were counted. Survival was expressed relative to the untreated control for each genotype. Each data point represents the mean CFU-S survival in ten recipient mice, expressed relative to untreated samples of the corresponding genotype.

Single HSC transplants. The single-stem-cell transplants were performed as described previously[39,40]. CD45.1 recipient mice (C57BL/6J × 129S6/Sv F1, 8-to-12-weeks old) were fed with water supplemented with the antibiotic enrofloxacin (Baytril, Bayer Corporation) for seven days before irradiation and for the duration of the experiment. The lethal radiation was delivered as a split dose of 1,000 rad (500 rad each, 3 h apart) using a ^{137}Cs GSR C1m source (GSR Gmbh).

The lethally irradiated recipients were injected with single HSCs sorted from *Aldh2*$^{-/-}$*Fancd2*$^{-/-}$ and control mice on a C57BL/6Jo1a × 129S4S6/Sv F1 background (CD45.2, 8-to-12 weeks old). Bone marrow cells from these mice were extracted with IMDM medium (GIBCO), filtered through a 70-μm strainer, spun down for 5 min at 1,200 r.p.m. and resuspended in 6 ml IMDM medium at room temperature. These cells were then overlaid onto 6 ml Lympholyte M (Cederlane) in a 15-ml Falcon tube and spun down for 20 min at 1,400*g* at room temperature with the brake off. The interface containing the mononucleated cells was transferred into another 15-ml tube and topped up with ice-cold MACS buffer (PBS pH 7.2, 0.5% BSA, 2 mM EDTA). After 5 min of centrifugation at 1,200 r.p.m., the cell pellets were resuspended in 320 μl of MACS buffer, stained with the lineage-depletion kit (130-090-858, MACS Miltenyi Biotec) following the manufacturer's instructions and passed through LS magnetic columns. Lineage-depleted cells were spun down for 5 min at 1,200 r.p.m. and the pellets were resuspended in 200 μl MACS buffer with the antibodies described previously (see Flow cytometry), except that anti-CD48 was directly conjugated to BV421 (clone HM48-1, BioLegend). The cells were resuspended in 500 μl of MACS buffer and run on a Synergy sorter (Sony Biotechnology Inc.).

Single HSCs, defined as lineage$^-$c-Kit$^+$Sca-1$^+$CD41$^-$CD48$^-$CD150$^+$, were sorted into 100 μl StemSpan SFEM medium (StemCell Technologies) in each well of a round bottom, 96-well plate (Costar) using a Synergy cell sorter (Sony Biotechnology). The plates were spun down for 5 min at 180*g* and the presence of a single cell per well was confirmed visually. The full content of selected wells was loaded into insulin syringes (29G, 0.5-inch needle) containing 2×10^5 carrier cells in 300 μl Hank's balanced salt solution (StemCell technlogies). The contents of the syringe were used to dislodge the single HSC from the bottom of the well, avoiding the creation of bubbles. The entire volume (400 μl) was injected into the tail veins of irradiated recipients and chimaerism was measured every 2 weeks using flow cytometry. Recipients were considered reconstituted by the single stem cell if chimaerism for CD45.2$^+$ WBCs was $\geq$ 0.1%.

Whole-genome sequencing of mouse HSC clones. Single HSCs were allowed to expand *in vivo* for four months to guarantee that the transplanted cell was a stem cell. Recipient mice that were positive for reconstitution were euthanized four months after transplantation, and the blood, bone marrow, spleen and thymus were collected. All tissues were prepared for flow cytometry as described above and stained with CD45.1 (FITC, clone A20, BioLegend) and CD45.2 (APC, clone 104, BioLegend) antibodies. CD45.2$^+$ cells were sorted from each tissue on a Synergy cell sorter (Sony Biotechnology), spun down and frozen at −80 °C. Genomic DNA was then extracted from the CD45.2$^+$ bone-marrow cells and from a tail biopsy that had been collected at 2 weeks of age from the same mouse that provided the single HSC. Genomic DNA was extracted with the Puregene Cell and Tissue kit (Qiagen) following the manufacturer's instructions.

Whole-genome sequencing was performed as described previously[41]. In brief, short-insert 500-bp genomic libraries were constructed according to Illumina library protocols and 100-base paired-end sequencing was performed on HiSeq 2000 or HiSeq X genome analysers to an average of 20× coverage. Short-insert paired-end reads were aligned to the reference mouse genome (NCBIM38) using BWA-MEM (http://bio-bwa.sourceforge.net/). For each HSC clone, the matched tail sample was used as the reference. We sequenced two of the *Aldh2*$^{-/-}$*Fancd2*$^{-/-}$ HSC clones to 40× coverage, together with their matched germ-line references. We noted a big overlap between the variants found at 20× and 40× coverage (data not shown), showing that doubling the coverage did not actually uncover many more mutations. Any additional calls found when the coverage was increased to 40× were predominantly subclonal, with a mean VAF of 0.22. Therefore, we concluded that 20× whole-genome sequencing provided sufficient coverage to allow us to uncover mutations present in the transplanted HSC.

Substitutions, indels and structural changes were called with the CaVEMan, Pindel and BRASS algorithms, which are described in detail elsewhere[42]. In addition to previously reported filtering[41], we asked that all variants were unique to each HSC clone and not found in unrelated HSC or tail samples, or in unrelated mouse strains. We did not apply a VAF filter for clonality because when we examined the VAF distribution of the final datasets, these were centered around 0.5 (Extended Data Fig. 9). For the transcriptional analysis, previously reported HSC RNA-seq data was aligned with Bowtie2 (http://bowtie-bio.sourceforge.net/bowtie2/index.shtml) against NCBIM38[43], and the overlap between indels and transcribed genes was calculated in R. To calculate the fraction of the genome covered by genes, positions of genes were retrieved from Ensembl. Overlapping regions between two genes were taken into account and counted only once.

Validation of indel and rearrangement calls. Indel calls of less than 50 bp were validated using multiplex PCR and targeted re-sequencing. We used 13 multiplex-primer combinations to capture and simultaneously amplify 172 (50%) of the previously identified indels. Primers were designed using MPprimer[44] to capture regions of between 190 and 250 bp in size (sequences available upon request). The first of round multiplex-PCR amplifications was performed with tailed gene primers and was individually barcoded by a second round of PCR with pre-validated MiSeq-ready primers[45], using a high fidelity polymerase (Q5 Hot Start HF, New England Biolabs). The PCR reaction conditions were as follows: Group 1, 100 ng DNA input in 25 μl PCR reaction, 95 °C for 2 min, six cycles of 98 °C for 20 s, 65 °C for 60 s, 60 °C for 60 s, 55 °C for 60 s, 50 °C for 60 s and 70 °C for 60 s, the reaction was then held at 4 °C until addition of barcoded second-round primers, followed by 19 cycles of 98 °C for 20 s, 62 °C for 15 s and 72 °C for 30 s, then 72 °C 60 s; Group 2, 10 ng DNA input in 5 μl PCR reaction, 95 °C for 2 min, seven cycles of 95 °C for 20 s, 58 °C for 17 min and 70 °C for 60 s, then held at 4 °C until addition of barcoded second-round primers, followed by 23 cycles of 98 °C for 20 s, 62 °C for 15 s and 72 °C for 30 s, then 72 °C 60 s. Each sample was pooled, size selected by SPRI (×0.8) and quantified before being stored at −20 °C until sequencing. Two MiSeq runs (300-bp paired-end) were used for variant confirmation, and reads were mapped with BWA. We analysed positions where the coverage was higher than 100× (159/172). With this approach, we were able to validate 91.2% of the original calls: 14/159 (8.8%) calls had VAF values <0.1 and were deemed false positives. The normal distribution of VAFs around 0.5 is consistent with most indels being clonal in origin.

For validation of rearrangements, we designed nested PCRs surrounding the breakpoints determined by the BRASS algorithm (primer sequences available upon request). PCR reactions were carried out in 20 μl, using 10 ng (HSC clones or tails) or 400 ng (donor bone marrow) of genomic DNA and GoTaq G2 Hot Start Polymerase (M7401, Promega). The first round of PCR amplifications was performed at 95 °C for 2 min, 35 cycles of 95 °C for 30 s, 55 °C for 20 s and 72 °C for 30 s, then 72 °C for 5 min. The reactions were diluted to 1 in 50 and 1 μl of the diluted reaction was used as template for a second round of PCR with nested primers, to increase specificity and sensitivity, performed at 95 °C for 2 min, 35 cycles of 95 °C for 30 s, 60 °C for 20 s and 72 °C for 30 s, then 72 °C for 5 min. The reactions were analysed on 2% agarose gels, bands of the expected sizes were excised and the identities of all products were confirmed by Sanger sequencing.

Using this approach, we found that 16/27 (59%) of rearrangements could be detected in the bone marrow of donor mice at the time the HSCs were transplanted (Extended Data Fig. 10). Any rearrangements present before transplantation must be clonal (that is, would not have arisen after the transplant). The failure to amplify the remaining 11 rearrangements by PCR does not mean that these are sub-clonal (that is, post-transplant) events. PCR amplification will depend on how much the transplanted HSC was contributing to blood production in the donor animal at the time of the transplant, as well as the sensitivity of each PCR. Therefore, we inferred clonality for the remaining calls by looking at loss of copy number (in the case of deletions, see Fig. 5l) and the number of reads involved in the rearrangement at the breakpoint for copy number-neutral changes.

Statistical analysis. Sample number (*n*) indicates the number of independent biological samples in each experiment. Sample numbers and experimental repeats are indicated in figure legends or Methods. Normality of data distribution was tested using the D'Agostino–Pearson omnibus normality test and variance was estimated before deciding on a statistical test. Unless otherwise stated in the

figure legend, data are shown as the mean ± s.e.m. and the two-sided nonparametric Mann–Whitney test was used to assess statistical significance. Analysis was performed using GraphPad Prism.

Data availability. Whole-genome sequencing data have been deposited in the EMBL European Nucleotide Archive (ENA) under the accession code ERP009447. All other data are available upon reasonable request from the authors.

30. Gu, Y. *et al.* Growth retardation and leaky SCID phenotype of Ku70-deficient mice. *Immunity* **7,** 653–665 (1997).
31. Farley, F. W., Soriano, P., Steffen, L. S. & Dymecki, S. M. Widespread recombinase expression using FLPeR (flipper) mice. *Genesis* **28,** 106–110 (2000).
32. de Boer, J. *et al.* Transgenic mice with hematopoietic and lymphoid specific expression of Cre. *Eur. J. Immunol.* **33,** 314–325 (2003).
33. Donehower, L. A. *et al.* Mice deficient for p53 are developmentally normal but susceptible to spontaneous tumours. *Nature* **356,** 215–221 (1992).
34. Giri, S. D. & Chatterjee, A. Modulation of mitomycin C-induced sister chromatid exchanges and cell cycle delay by buthionine sulfoximine and reduced glutathione in mouse bone marrow cells *in vivo*. *Mutat. Res.* **413,** 227–234 (1998).
35. Orsburn, B. *et al.* Differential requirement for H2AX and 53BP1 in organismal development and genome maintenance in the absence of poly(ADP)ribosyl polymerase 1. *Mol. Cell. Biol.* **30,** 2341–2352 (2010).
36. Geigl, J. B., Uhrig, S. & Speicher, M. R. Multiplex-fluorescence in situ hybridization for chromosome karyotyping. *Nat. Protoc.* **1,** 1172–1184 (2006).
37. Gribble, S. M. *et al.* Massively parallel sequencing reveals the complex structure of an irradiated human chromosome on a mouse background in the Tc1 model of Down syndrome. *PLoS ONE* **8,** e60482 (2013).
38. Reinholdt, L., Ashley, T., Schimenti, J. & Shima, N. Forward genetic screens for meiotic and mitotic recombination-defective mutants in mice. *Methods Mol. Biol.* **262,** 87–107 (2004).
39. Kent, D., Dykstra, B. & Eaves, C. Isolation and assessment of long-term reconstituting hematopoietic stem cells from adult mouse bone marrow. *Curr. Protoc. Stem Cell Biol.* (2007).
40. Oguro, H., Ding, L. & Morrison, S. J. SLAM family markers resolve functionally distinct subpopulations of hematopoietic stem cells and multipotent progenitors. *Cell Stem Cell* **13,** 102–116 (2013).
41. Behjati, S. *et al.* Genome sequencing of normal cells reveals developmental lineages and mutational processes. *Nature* **513,** 422–425 (2014).
42. Nik-Zainal, S. *et al.* The genome as a record of environmental exposure. *Mutagenesis* **30,** 763–770 (2015).
43. Cabezas-Wallscheid, N. *et al.* Identification of regulatory networks in HSCs and their immediate progeny via integrated proteome, transcriptome, and DNA methylome analysis. *Cell Stem Cell* **15,** 507–522 (2014).
44. Shen, Z. *et al.* MPprimer: a program for reliable multiplex PCR primer design. *BMC Bioinformatics* **11,** 143 (2010).
45. Quail, M. A. *et al.* A large genome center's improvements to the Illumina sequencing system. *Nat. Methods* **5,** 1005–1010 (2008).
46. Krishna, G., Fiedler, R. & Theiss, J. C. Simultaneous evaluation of clastogenicity, aneugenicity and toxicity in the mouse micronucleus assay using immunofluorescence. *Mutat. Res.* **282,** 159–167 (1992).

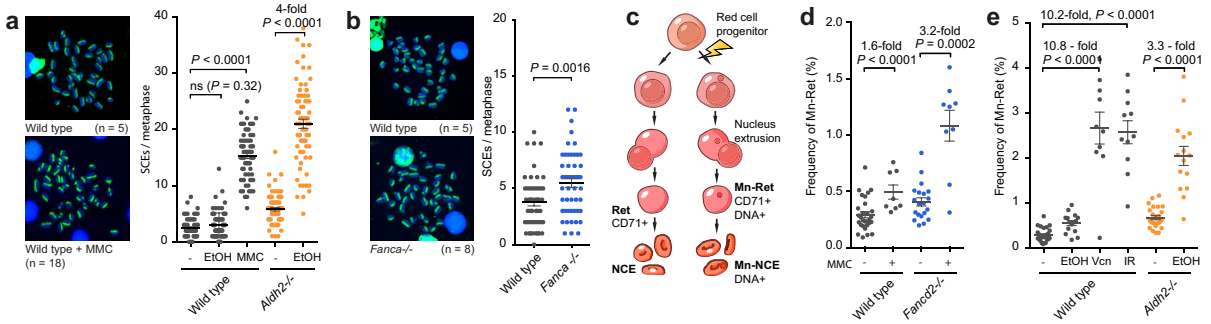

f Untreated

Wild type	0/30	
	0/30	
	0/30	
Aldh2$^{-/-}$	0/30	
	0/30	
	2/30	40,XX, Del(2)
		40,XX, Del(13)
Fancd2$^{-/-}$	0/30	
	1/30	40,XY, Chtb(X), Chtb(4)
	2/30	40,XY, Chtb(2)
		40,XY, Chtb(5)
Aldh2$^{-/-}$*Fancd2*$^{-/-}$	7/30	40,XY, Der(X)T(X;2), Der(2)T(X;2)
		40,XY, T(12;17), Dp(16), Del(16)
		40,XY, Der(8)T(8;14)
		40,XY, Dp(2)
		40,XY, Dp(2),Chtb(1)
		40,XY, Del(6)
		40,XY, Der(1)T(1;5), Der(5)T(1;5), Der(13)T(2;13)
	2/30	40,XY, Dp(16)
		40,XY, Chtb(X)
	2/30	40,XY, Del(2)
		39,XY, -19, Rb(12;19)

g 48 hours after Ethanol IP (5.8 g/kg)

Wild type	2/30	39,X,-Y		
		39,X,-Y		
	0/30			
	0/30			
Aldh2$^{-/-}$	0/30			
	0/30			
	1/30	41,XX,+9, Chtb(9)		
Fancd2$^{-/-}$	4/30	40,XY, Chtb(4)	1/30	40, XY, Chtb(17)
		40,XY, Chte(11;4)x1	2/30	41,XX, +12
		41,XY, +11		40,XX, Chtb(12)
		41,XY, +7		
Aldh2$^{-/-}$*Fancd2*$^{-/-}$	22/30	40,XY, Del(13)		40,XX, Chtb(5)
		39,XY, -8, Del(2),T(8;15)		40,XX, Chtb(1)
		40,XY, -1, Del(7),Del(17),+Del(15)		39,XX, -12,Del(4), Der(7)t(7;15), Der(15)t(7;15)
		40,XY, -2, +T(3;11)		40,XX, Del(2), Chtb(7)
		40,Y, Del(X), Del(6),T(7;11)		40,XX, Chtb(19)
		40,XY, Del(1), Der(13)T(2;13)		40,XX, Del(X)
		40,XY, Chte(5;18)x2, Chte(2;12)		40,XX, Del(7), Chtb(1); Chtb(9); Chtb(16)
		40,XY, Chte(9;17), Del(5), Chtb(8), Chtb(9)		39,XX, -11, Del(10), Der(14)T(10;14)
		40,XY, Chte(13;14), Chtb(3)		40,XX, Del(4)
		40,XY, -9, Chtb(15)		40,XX, Chtb(1)
		40,XY, Del(12), Chtb(7), Chtb(12), Chtb(13)		40,XX, Del(1)
		40,XY, Del(2), Der(17)T(16;17), Chtb(10)	15/30	39,XX, Der(8)T(8;18), Der(10;19)
		40,XY, Dp(4), Del(5), Chtb(2)		40,XX, Del(5),Der(8)T(8;16), Chtb(X)
		40,XY, Del(X), Chtb(4)		40,XX, Del(14), Der(18)T(6;18)
		40,XY, Del(5), Chtb(14)		40,XX, Del(6)
		41,XY, -6, +15, Del(14), Chtb(15), Der(X)T(6;X)		40,XX, Chtb(2)
		40,XY, Chtb(1),Chtb(14)		40,XX, T(X;7), Del(2)
		40,XY, Chtb(12)		40,XX, -6, +Del(17), Chtb(14)
		40,XY, Chtb(6)		40,XX, -17, +Del(2), Der(2)T(2;17)
		40,XY, Chtb(4)		40,XX, Del(7),+14, Chtb(16)
		40,XY, Chtb(9)		40,XX, Der(7)T(4;7),+Del(8),…
		40,XY, Chtb(6)		…Chtb(1), Chtb(2), Chtb(15)
	17/30	40,XX, Der(6)T(1;6)		40,XX, Del(X),Der(3)T(3;10),…
		40,XX, Del(12)		…Der(10)T(3;10), Chtb(2), Chtb(3), Chtb(10)
		40,XX, Chte(4;7)x2		39,XX, -1, Der(12)T(9;12)
		40,XX, Del(6), Der(12)T(6;12)		40,XX, Del(10), Chtb(6)
		40,XX, Del(2), Chtb(13)		40,XX, Der(3;19), -19
		40,XX, Del(13), Der(16)T(1;16)		40,XX, -10, dic(18;18)

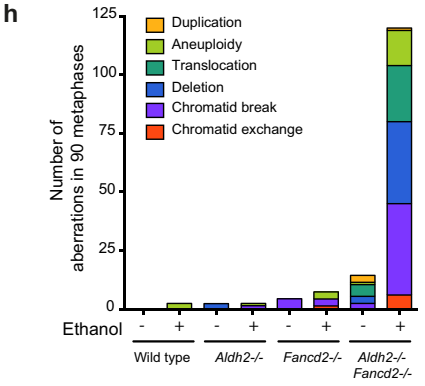

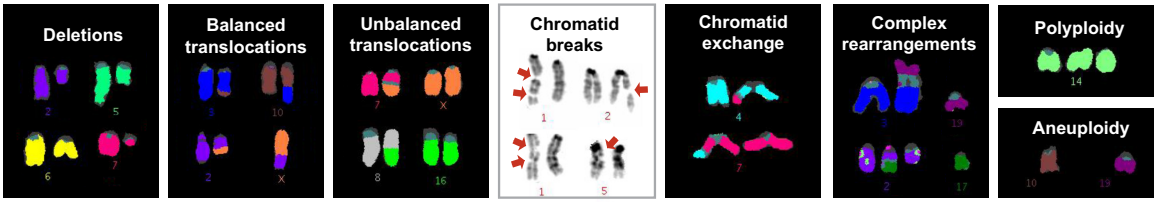

Extended Data Figure 1 | See next page for caption.

Extended Data Figure 1 | Ethanol-induced genomic instability. **a**, Left, representative images of bone marrow metaphase spreads from wild-type mice treated with mitomycin C (MMC); *n* shows the number of SCE events per metaphase. Right, comparison between number of SCEs in the bone marrow of wild-type and *Aldh2*$^{-/-}$ mice treated with ethanol (5.8 g kg^{-1}) or MMC (1 mg kg^{-1}). Triplicate experiments, 25 metaphases per mouse, $n = 75$; *P* calculated by two-sided Mann–Whitney test; data shown as mean and s.e.m. Ethanol causes a strong homologous recombination response in *Aldh2*$^{-/-}$ mice, comparable to that observed in wild-type mice exposed to MMC. **b**, Left, representative images of bone marrow metaphase spreads from wild-type and *Fanca*$^{-/-}$ mice; *n* shows the number of SCE events per metaphase. Right, quantification of SCEs (duplicate experiments, 25 metaphases per mouse, $n = 50$; *P* calculated by two-sided Mann–Whitney test; data shown as mean and s.e.m.). Mice deficient in cross-link repair (*Fanca*$^{-/-}$, or *Fancd2*$^{-/-}$ in Fig. 1a) show a small but significant increase in the number of spontaneous SCE events, indicating that a homologous recombination repair response occurs in the absence of the Fanconi anaemia pathway. **c**, Scheme depicting the formation of micronucleated erythrocytes. Micronuclei (Mn) generated by fragmentation or mis-segregation of chromosomes during erythrocyte maturation remain in the erythrocyte after extrusion of the main nucleus. These fragments can be detected by a DNA stain (PI^{+}). During maturation, red-cell progenitors lose CD71 expression. Therefore, peripheral CD71^{+} red cells represent immature, short-lived reticulocytes (Ret) and CD71^{-} cells represent mature, long-lived normochromic erythrocytes (NCEs). **d**, Proof-of-principle experiment showing the induction of micronucleated reticulocytes 48 h after MMC treatment (1 mg kg^{-1}). *P* calculated by two-sided Mann–Whitney test; data shown as mean and s.e.m.; $n = 29$, 8, 20 and 9 mice, left to right. **e**, Treatment of *Aldh2*$^{-/-}$ mice with ethanol (5.8 g kg^{-1}) leads to potent micronucleus formation. This induction is comparable to that observed in wild-type mice that were treated with the aneugen vincristine (Vcn, 0.2 mg kg^{-1}, 48 h) or clastogenic γ-irradiation (IR, 400 rad, 48 h)[46]. *P* calculated by two-sided Mann–Whitney test; data shown as mean and s.e.m.; $n = 29$, 15, 10, 11, 25 and 15 mice. **f**, List of chromosomal aberrations observed in the bone marrow of 8-to-12-week-old untreated *Aldh2*$^{-/-}$*Fancd2*$^{-/-}$ and control mice. **g**, List of chromosomal aberrations observed in the bone marrow of 8-to-12-week-old *Aldh2*$^{-/-}$*Fancd2*$^{-/-}$ and control mice 48 h after ethanol treatment (5.8 g kg^{-1}, injected intraperitoneally, IP). In **f** and **g**, three mice and 30 metaphases per mouse were analysed per condition, and the numbers represent the fraction of abnormal metaphases per mouse. **h**, Bar chart classifying the type of aberrations for each genotype (90 metaphases per condition). **i**, Examples of different types of chromosomal aberrations.

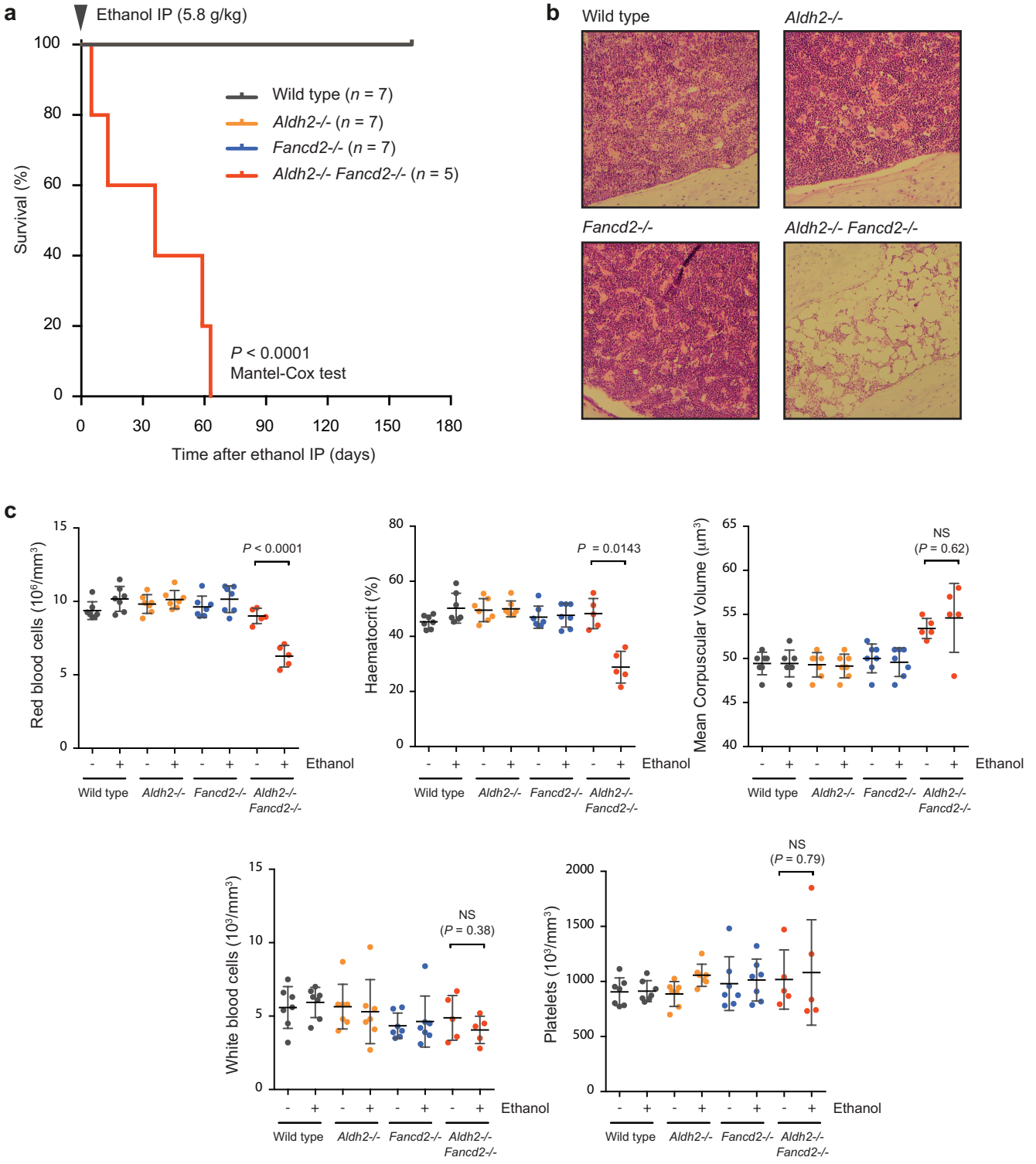

Extended Data Figure 2 | A single dose of ethanol precipitates bone-marrow failure in *Aldh2*$^{-/-}$*Fancd2*$^{-/-}$ mice. a, A single dose of ethanol (5.8 g kg^{-1}, injected intraperitoneally) leads to anaemia in *Aldh2*$^{-/-}$*Fancd2*$^{-/-}$ mice one to two months after treatment (*P* calculated by Mantel-Cox test; *n* = number of mice). **b**, Haematoxylin and eosin staining of bone marrow sections 30 days after ethanol treatment (original magnification, ×100). **c**, Full blood-count analysis for *Aldh2*$^{-/-}$*Fancd2*$^{-/-}$ and control mice, before injection and terminal bleeds after ethanol treatment (*P* calculated by paired *t*-test; data shown as mean and s.e.m.; *n* = number of mice, as in **a**).

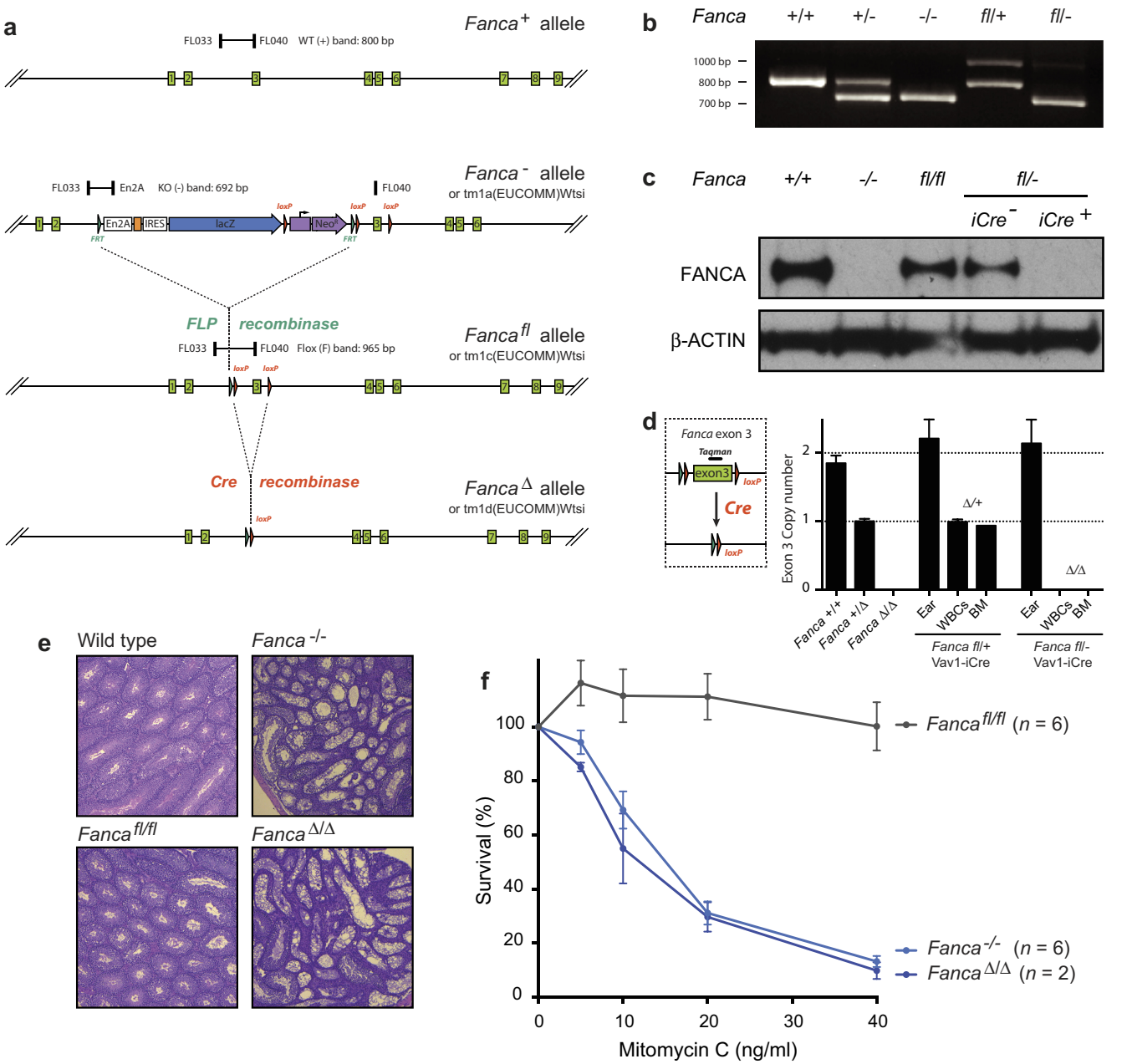

Extended Data Figure 3 | Generation of a conditional *Fanca* allele. **a**, Mice carrying the previously reported *Fanca*$^{-}$ allele (*Fanca*$^{tm1a(EUCOMM)Wtsi}$) were crossed with mice carrying the FLP recombinase, yielding the *Fanca*^{fl} allele (*Fanca*$^{tm1c(EUCOMM)Wtsi}$). This allele restores FANCA expression as shown by western blot (Fig. 3). Cre-mediated recombination of *Fanca*^{fl} yields the *Fanca*$^{\Delta}$ allele (*Fanca*$^{tm1d(EUCOMM)Wtsi}$), which lacks exon 3 and leads to loss of FANCA protein (Fig. 3). **b**, Genotyping PCRs for the wild-type, *Fanca*$^{-}$ and *Fanca*^{fl} alleles with primers FL033, FL040 and En2A; showing bands of the expected sizes. **c**, Western blot (single experiment) showing complete absence of FANCA protein in the spleens of *Fanca*$^{-/-}$ and *Fanca*$^{fl/-}$ *Vav1*-iCre mice. For gel source data, see Supplementary Fig. 1. **d**, Determination of the number of exon 3 copies by quantitative PCR. Wild-type, *Fanca*$^{+/\Delta}$ *and Fanca*$^{\Delta/\Delta}$ mice carry 2, 1 and 0 copies, respectively. *Fanca*^{fl} *Vav1*-iCre mice show tissue-specific deletion of exon 3 in white blood cells (WBCs) and bone marrow ($n = 4$ technical replicates; bars: mean, s.d.). **e**, Microscopic analysis of haematoxylin and eosin-stained sections of testes (original magnification, ×50) from wild-type, *Fanca*$^{-/-}$, *Fanca*$^{fl/fl}$ and *Fanca*$^{\Delta/\Delta}$ males at 12 weeks, showing impaired spermatogenesis in testes of *Fanca*$^{-/-}$ and *Fanca*$^{\Delta/\Delta}$ mice (one experiment). **f**, Sensitivity assay of transformed mouse-embryonic fibroblasts (MEFs) derived from *Fanca*$^{-/-}$, *Fanca*$^{fl/fl}$ and *Fanca*$^{\Delta/\Delta}$ embryos, showing hypersensitivity of both *Fanca*$^{-/-}$ and *Fanca*$^{\Delta/\Delta}$ cells to the cross-linking agent mitomycin C (n = number of experiments, each carried out in quadruplicate; bars: mean, s.e.m.).

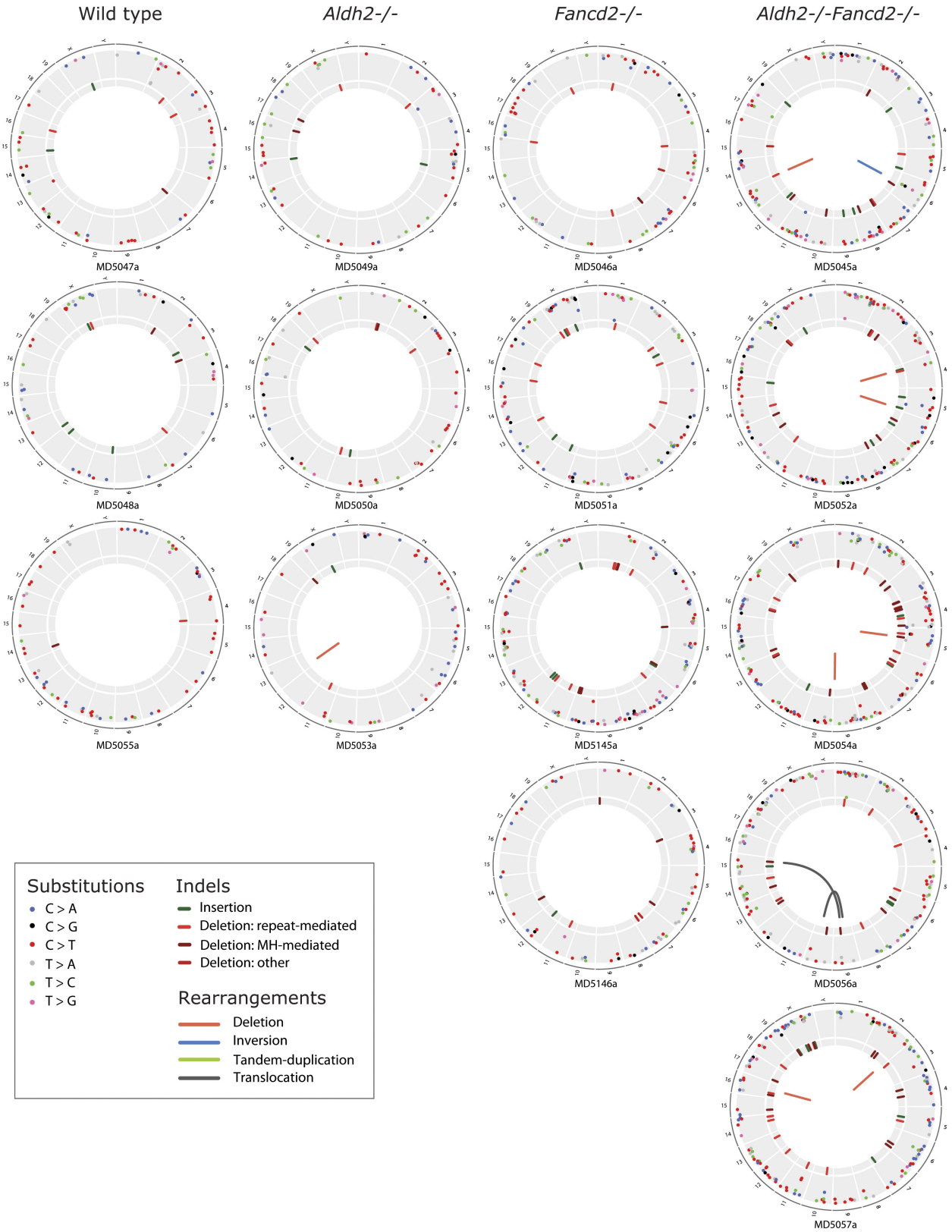

Extended Data Figure 4 | Endogenous aldehydes mutate the HSC genome. Circos plots showing the mutations observed in all sequenced HSC clones (wild type, $n = 3$; *Aldh2*$^{-/-}$, $n = 3$; *Fancd2*$^{-/-}$, $n = 4$; and *Aldh2*$^{-/-}$*Fancd2*$^{-/-}$, $n = 5$ HSC genomes). Substitutions, indels and rearrangements are plotted.

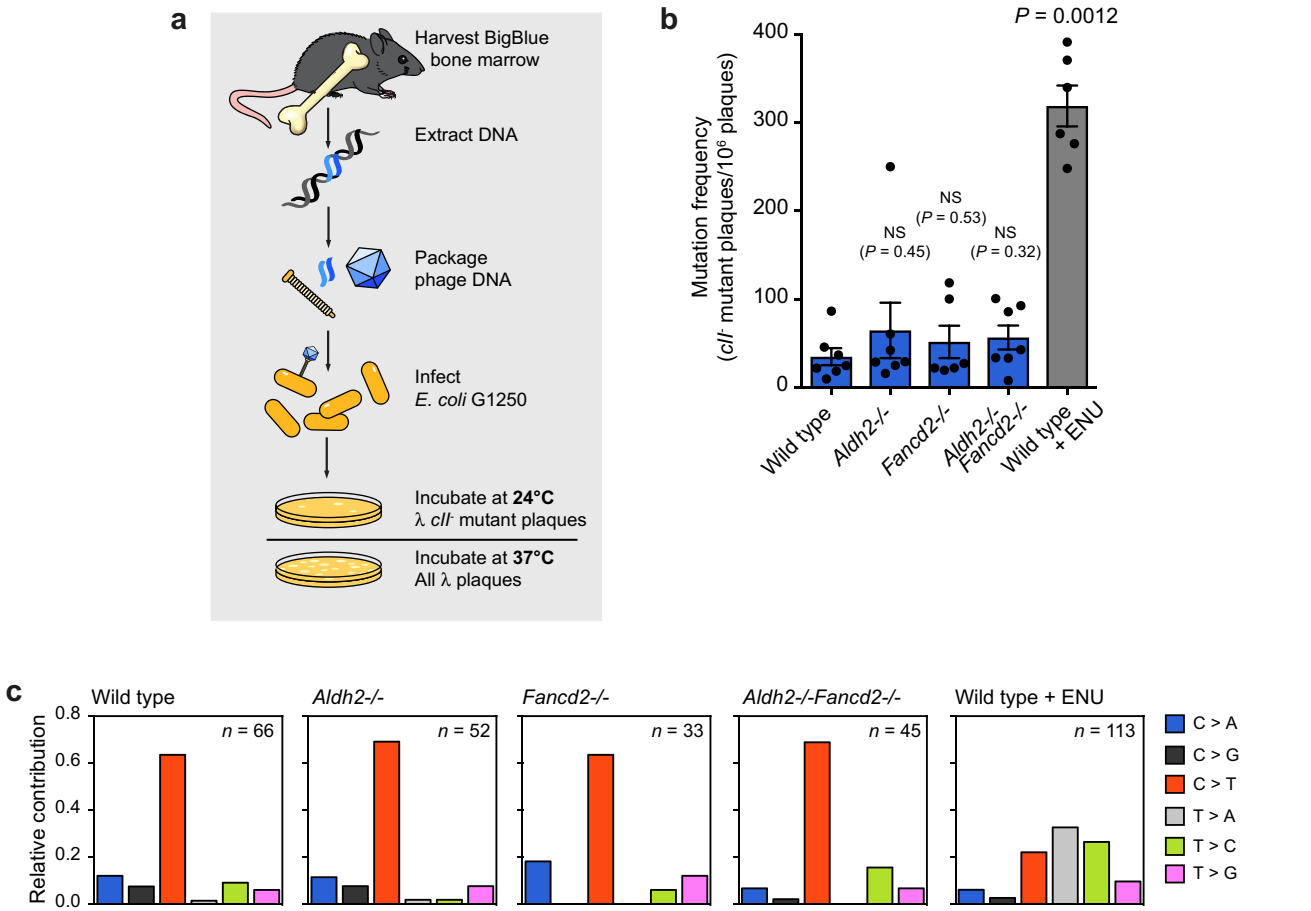

Extended Data Figure 5 | Detection of point mutations in mice with the BigBlue reporter system. a, Chromosome 4 of the BigBlue reporter mouse harbours a λ-phage transgene that contains the mutational target. The phage DNA can be recovered from mouse tissues, packaged into phage and used to infect bacteria. Phage *cII* mutants can be detected by the ability of these phage to form plaques at 24 °C. **b**, Quantification of the frequency of cII^{-} -mutant phage recovered from the bone marrow of young $Aldh2^{-/-}Fancd2^{-/-}$ and control mice carrying the BigBlue transgene. ENU-treated mice serve as positive controls for the assay (*P* calculated by two-sided Mann–Whitney test; data shown as mean and s.e.m.; $n = 7, 7, 6, 7$ and 6 mice, left to right). **c**, Relative contribution of the indicated mutation classes to the point-mutation spectra of cII^{-}-mutant phage isolated from the bone marrow. The ENU-mutation spectrum is characterized by T to A transversions and T to C transitions. *n* is the number of sequenced cII^{-} mutant phage.

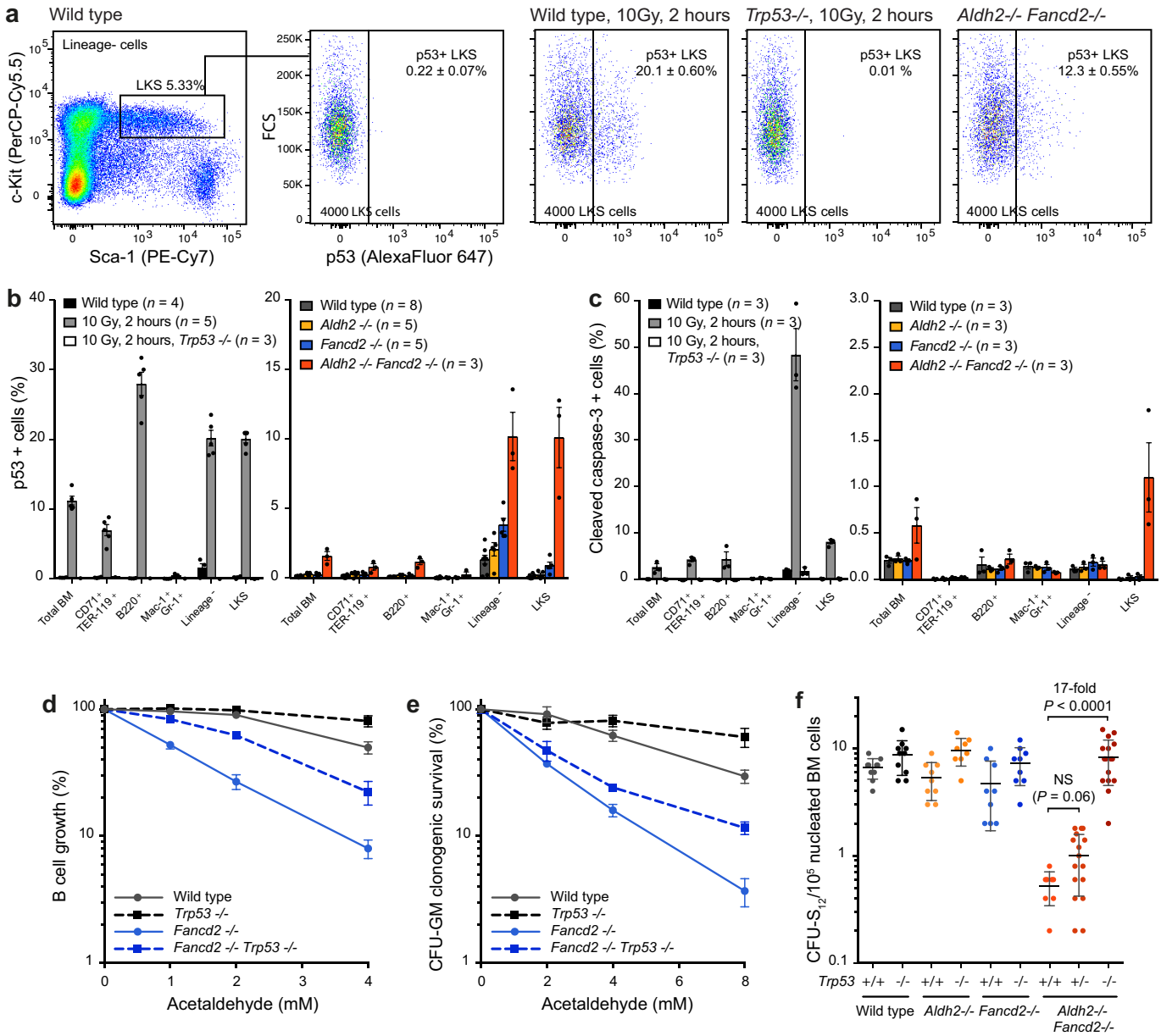

Extended Data Figure 6 | Aldehyde-induced stress elicits a p53 response. a, Representative flow cytometry plots for the quantification of $p53^+$ LKS cells from 8-to-12-week-old $Aldh2^{-/-}Fancd2^{-/-}$ and control mice. Cells were collected from wild-type and $Trp53^{-/-}$ mice 2 h after 10 Gy irradiation as positive and negative controls, respectively, for the assay. **b**, Quantification of the frequency of $p53^+$ cells in different bone-marrow populations. **c**, Quantification of the frequency of cleaved-caspase-3^+ cells in different bone marrow populations by flow cytometry. In **b** and **c**, irradiated wild-type and $Trp53^{-/-}$ mice were used as controls. Owing to the low numbers of LKS $CD48^-$ $CD150^+$ cells in $Aldh2^{-/-}Fancd2^{-/-}$ mice, the number of $p53^+$ or cleaved-caspase-3^+ HSCs could not be determined (data shown as mean and s.e.m.; n = number of mice). **d**, **e**, Survival of B cells and myeloid progenitors (CFU-GM) following exposure to acetaldehyde *in vitro*. Cells were obtained from $Fancd2^{-/-}Trp53^{-/-}$ and control mice. Each point represents the mean of three independent experiments, each carried out in quadruplicate; data shown as mean and s.e.m. **f**, Frequency of CFU-S_{12} in the bone marrow of $Aldh2^{-/-}Fancd2^{-/-}Trp53^{-/-}$ and control mice. Each point represents the number of CFU-S_{12} in the spleen of a single recipient (P calculated by two-sided Mann–Whitney test; data shown as mean and s.e.m.; n = 10–15 mice).

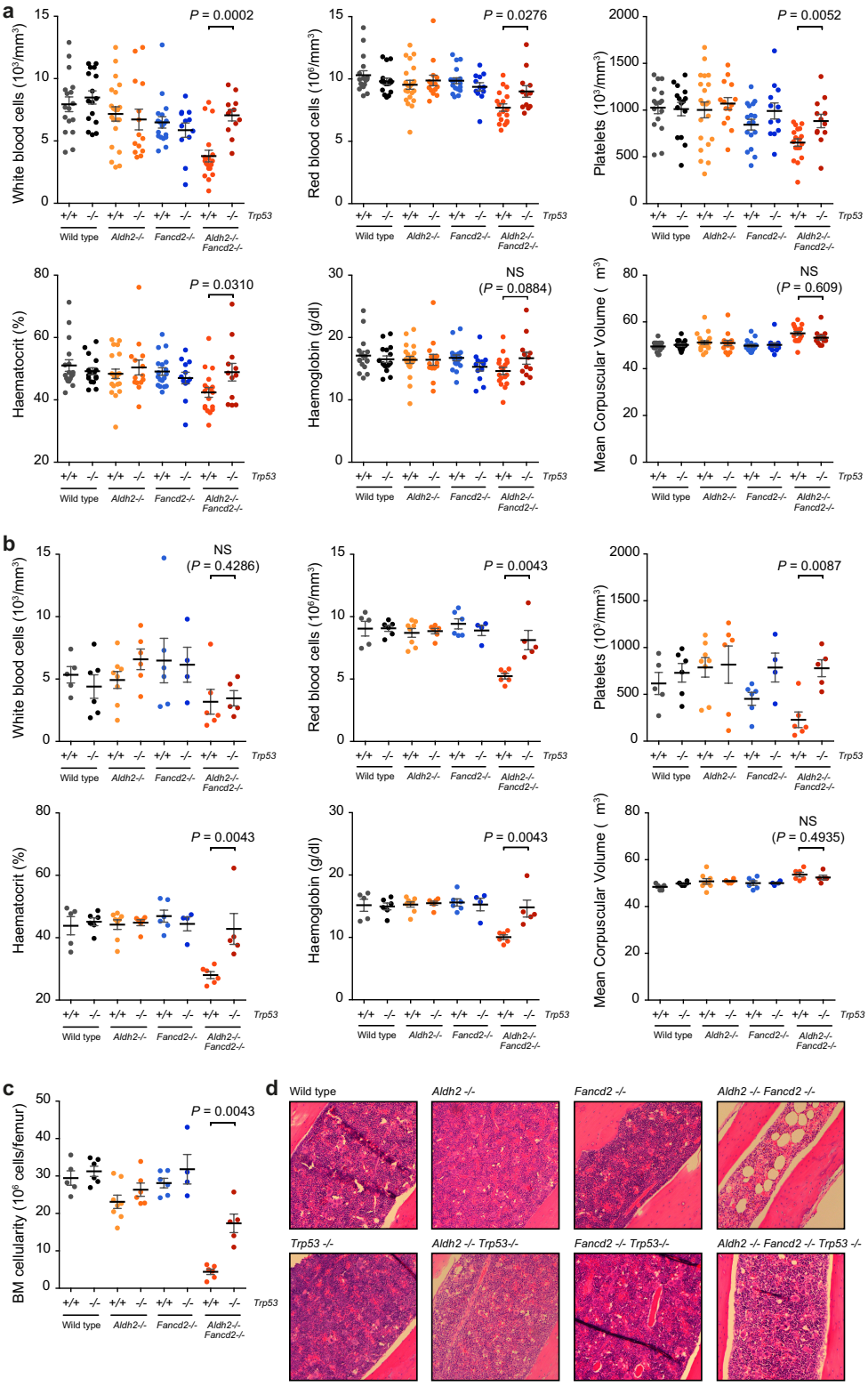

Extended Data Figure 7 | p53 deficiency suppresses peripheral-blood cytopenias and ethanol-induced bone-marrow failure in *Aldh2*$^{-/-}$*Fancd2*$^{-/-}$ mice. a, Full blood count analysis of *Aldh2*$^{-/-}$*Fancd2*$^{-/-}$*Trp53*$^{-/-}$ and control mice (8-to-12 weeks old, on a C57BL/6 × 129S4S6/Sv F1 background). A significant increase in the number of white blood cells, red blood cells, platelets and haematocrit was observed in *Aldh2*$^{-/-}$*Fancd2*$^{-/-}$*Trp53*$^{-/-}$ mice compared to *Aldh2*$^{-/-}$*Fancd2*$^{-/-}$ mice (*P* calculated by two-sided Mann–Whitney test; data shown as mean and s.e.m.; $n = 17, 16, 21, 14, 18, 12, 18$ and 12 mice, left to right). **b**, *Aldh2*$^{-/-}$*Fancd2*$^{-/-}$, *Aldh2*$^{-/-}$*Fancd2*$^{-/-}$*Trp53*$^{-/-}$ and control mice were treated with ethanol in their drinking water for 10 days as described previously[6]. Full blood-count analyses were carried out after 10 days of ethanol treatment. **c**, Bone marrow cellularity after 10 days of ethanol treatment. In **b**, **c**, *P* calculated by two-sided Mann–Whitney test; data shown as mean and s.e.m.; $n = 5, 6, 8, 6, 6, 4, 6$ and 5 mice, left to right. **d**, Haematoxylin and eosin staining of bone-marrow sections 10 days after ethanol treatment (original magnification, ×100).

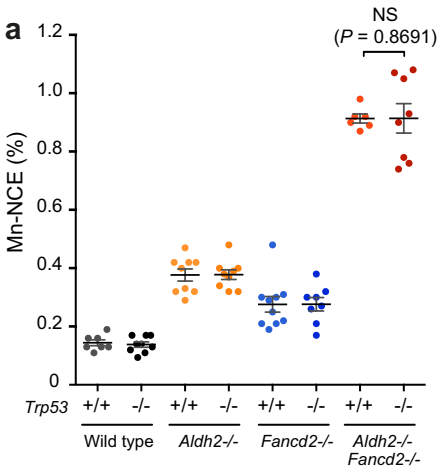

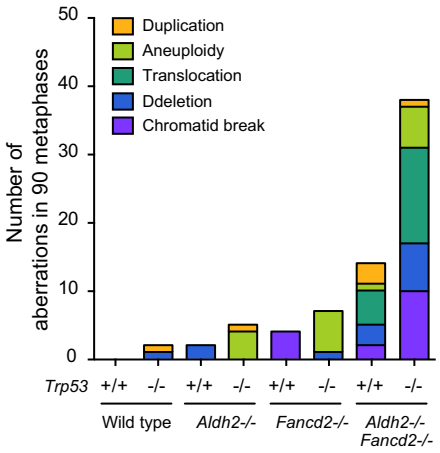

b

Trp53$^{-/-}$	**1/30**	40,XY ,Dp(Y)
	1/30	40,XY, Del(9)
	0/30	
Aldh2$^{-/-}$ *Trp53*$^{-/-}$	**0/30**	
	1/30	40,XX, Dp(9)
	4/30	39,X, -Y [x2]
		39,XY, -19 [x2]
Fancd2$^{-/-}$ *Trp53*$^{-/-}$	**3/30**	42,XX, +4,+6 [x2]
		41,XX, +6
	2/30	39,X,-X [x2]
	1/30	40,XX, Del(10)

Aldh2$^{-/-}$*Fancd2*$^{-/-}$ *Trp53*$^{-/-}$	**11/30**	40,XY, der(3)T(2;3)
		40,XY, Del(10)
		40,XY, T(5;7)
		40,XY, der(12)T(12;17), Del(17)
		39,XY, der(3)T(3;?),der(13)T(13;18)
		41,XY, +4 [x2]
		41,XY, Del(2),+8
		40,XY, T(2;13)
		40,XY, der(2)T(2;18)
		40,XY, Del(2)
	11/30	39,XY, der(2)T(2;11)
		40,XY, der(2)T(2;4), Del(4)
		40,XY, Dp(1)
		40,XY, der(9)T(4;9) [x2]
		40,XY, Del(1), Del(15)
		40,XY, Del(1)
		40,XY, Del(6)
		40,XY, Del(Y)
		41,XY, Chrb(3)
		39,XY, -10, Del(14)
	6/30	40,XY, T(13,16)
		40,XY, Del(19)
		39,XY, der(11)T(X;11), -1
		40,XY, T(10;16)
		40,XY, T(3;11)
		40,XY, Chrb(5)

d

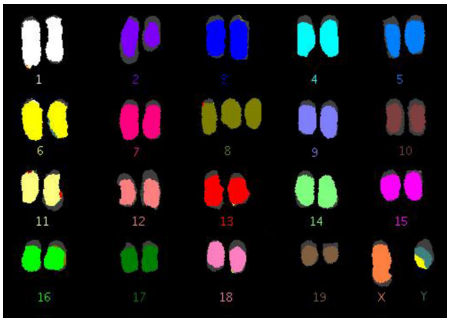

41,XY, Del(2),+8

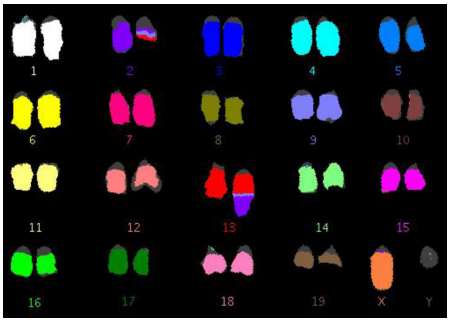

40,XY, T(2;13)

Extended Data Figure 8 | Genomic instability in *Aldh2*$^{-/-}$*Fancd2*$^{-/-}$*Trp53*$^{-/-}$ mice. a, Quantification of micronucleated NCEs in the blood of *Aldh2*$^{-/-}$*Fancd2*$^{-/-}$*Trp53*$^{-/-}$ and control mice (*P* calculated by two-sided Mann–Whitney test; data shown as mean and s.e.m.; $n = 8$ mice). **b**, List of chromosomal aberrations observed in the bone marrow of 8-to-12 week-old untreated *Aldh2*$^{-/-}$*Fancd2*$^{-/-}$*Trp53*$^{-/-}$ and control mice. Three mice and 30 metaphases per mouse were analysed per genotype; the numbers represent the fraction of abnormal metaphases per mouse. **c**, Bar chart classifying the types of aberrations for each genotype (90 metaphases per condition). **d**, Examples of two metaphases from an *Aldh2*$^{-/-}$*Fancd2*$^{-/-}$*Trp53*$^{-/-}$ mouse.

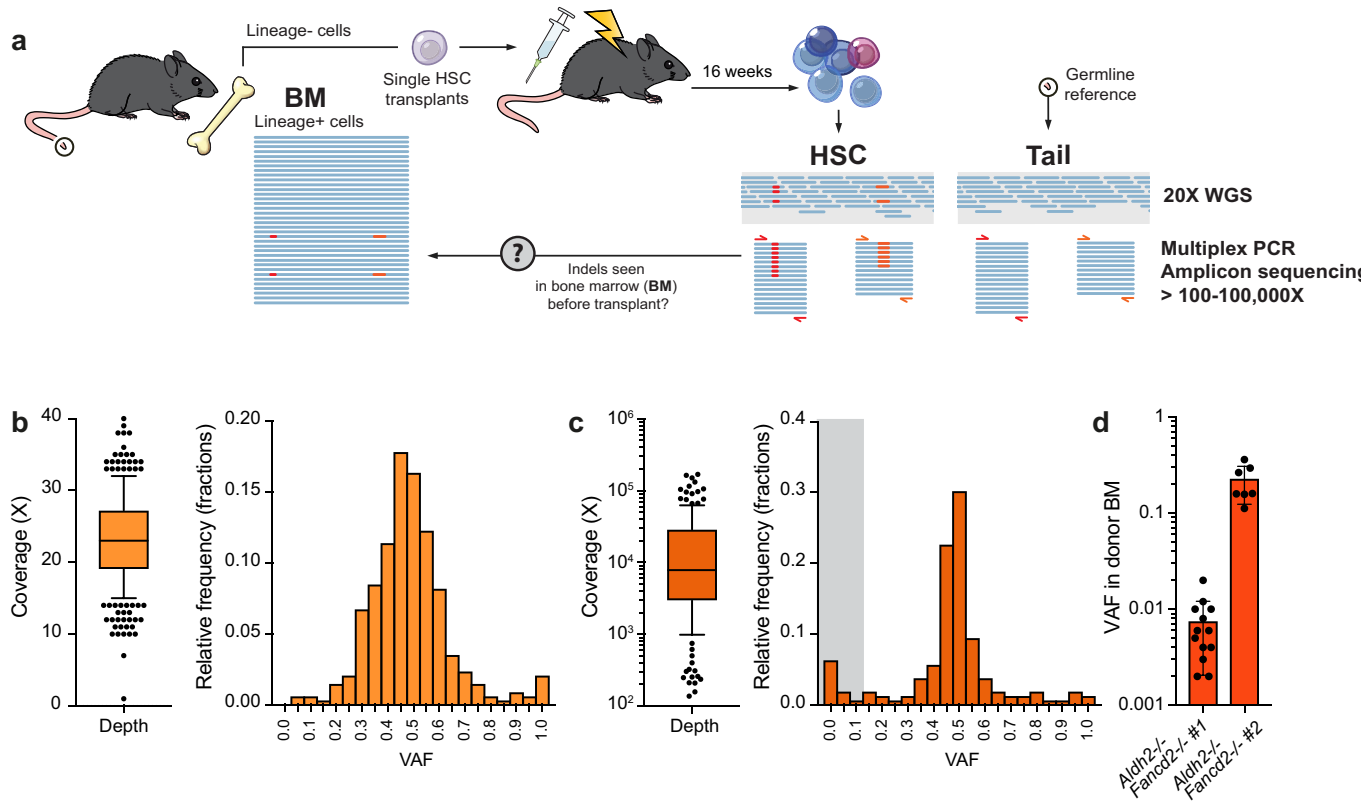

Extended Data Figure 9 | Validation of indels by targeted deep sequencing. a, Scheme depicting the generation of HSC clones by transplantation of single stem cells, subsequent whole-genome sequencing and validation of indel calls by amplicon deep sequencing. On the basis of the indel location from 20× whole-genome sequencing, we designed multiplex PCRs and deep sequenced the PCR products to higher coverage (100–100,000×) to confirm that the calls were not sequencing artefacts. In addition, we attempted to detect indels in DNA samples of bone-marrow cells from the mice that provided the transplanted HSCs. **b**, Coverage depth and VAF of the filtered set of indel calls from whole-genome sequencing ($n = 342$ indels; box plot shows the mean, box edges represent the first and third quartiles, whiskers extend over 10–90% of data). **c**, Coverage depth and VAF of the indel calls from deep sequencing validation ($n = 159$ locations; box plot shows the mean, box edges represent the first and third quartiles, whiskers extend over 10–90% of data). One hundred and fifty-nine locations had coverage greater than 100× and were used for the analysis. We could validate the presence of 91.2% of the initial calls; 14/159 (8.8%) calls had VAF <0.1 and were deemed false positives (indicated by grey shading). Note that the VAF distribution is centred tightly around 0.5, confirming the clonal nature of most indels. **d**, We used targeted deep sequencing to look for indel calls in bone-marrow samples from the mice that provided the transplanted HSCs. In most cases, the calls were below the detection limit of the assay (VAF <0.0001). However, we could detect indels from two *Aldh2*$^{-/-}$*Fancd2*$^{-/-}$ HSCs, indicative of 'clonal haematopoiesis' in these mice (accounting for 0.7 and 21.4% of blood production, respectively). Data shown as mean and s.e.m.; $n = 13$ and 7 indels.

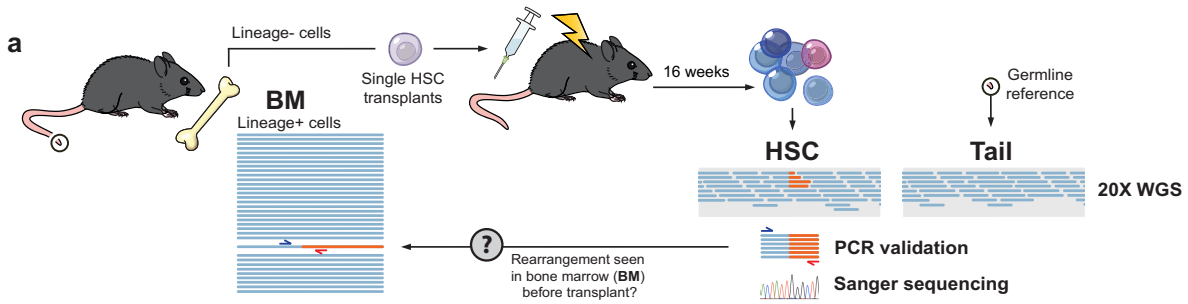

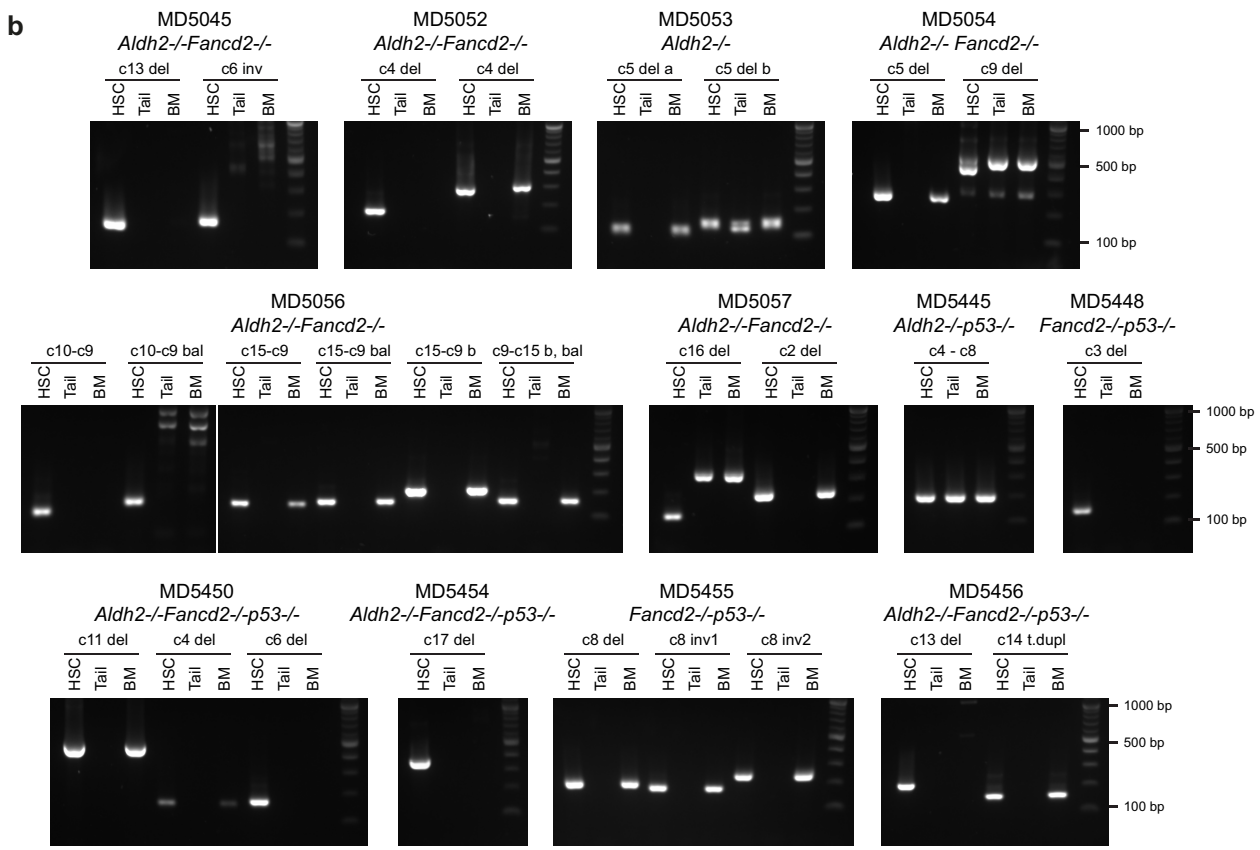

c

Sample	Type	Start location	Size (bp)	PCR	HSC	Tail	BM
MD5045a	deletion	c13:112244133	2999	161	●		
Aldh2-/- Fancd2-/-	inversion	c6:69207252	36822	135	●		
MD5052a	deletion	c4:29837258	9957	173	●		
Aldh2-/- Fancd2-/-	deletion	c5:145424065	24239	336	●		●
MD5053a	deletion	c13:19185501	24841	103	●		●
Aldh2-/-	deletion	c13:19311304	25273	132	●		●
MD5054a	deletion	c5:59377956	1148	268	●		●
Aldh2-/- Fancd2-/-	deletion/duplication	c9:117677119	342	198	●		
MD5056a	translocation	c10:82901864-c9:49792783	-	169	●		
Aldh2-/- Fancd2-/-	translocation (bal)	c10:82901948-c9:49793011	-	161	●		
	translocation	c15:80199437-c9:77318662	-	152	●		●
	translocation (bal)	c15:80199443-c9:77318664	-	163	●		●
	translocation	c15:80200657-c9:77317682	-	226	●		●
	translocation (bal)	c15:80200668-c9:77317689	-	176	●		●
MD5057a	deletion	c16:56319262	10056	131	●		
Aldh2-/- Fancd2-/-	deletion	c2:177355146	3657	229	●		●

Sample	Type	Start location	Size (bp)	PCR	HSC	Tail	BM
MD5445a	translocation	c4:128611975-c8:106880788	-	199	●	●	●
Aldh2-/- p53-/-							
MD5448a	deletion	c3:81290371	10604	167	●		
Fancd2-/- p53-/-							
MD5450a	deletion	c11:37239409	6950	477	●		●
Aldh2-/- Fancd2-/- p53-/-	deletion	c4:124986607	24307	164	●		●
	deletion	c6:86545624	47656	177	●		
MD5454a	deletion	c17:46760471	88447	321	●		
Aldh2-/- Fancd2-/- p53-/-							
MD5455a	deletion	c8:44991181	7530	191	●		●
Fancd2-/- p53-/-	inversion	c8:45073529	72375	180	●		●
	inversion	c8:45070602	69445	244	●		●
MD5456a	deletion	c13:84517083	54157	212	●		
Aldh2-/- Fancd2-/- p53-/-	duplication	c14:64748311	1651	153	●		●

Extended Data Figure 10 | Validation of rearrangements by PCR. **a**, Scheme depicting the generation of HSC clones by transplantation of single stem cells, subsequent whole-genome sequencing and validation of rearrangement calls by PCR. We designed primers for nested PCRs flanking the breakpoints calculated by the BRASS algorithm, and the identity of the products was confirmed by Sanger sequencing. In addition, we attempted to detect the rearrangements in DNA samples of bone-marrow cells from the mice that provided the transplanted HSCs, demonstrating that these changes did not arise during clonal expansion and were present in the stem cell at the time of transplantation. **b**, Agarose gels (one experiment) showing presence of specific PCR amplification from DNA of HSC clones, absence in matched germline samples from the tail of the same mouse and, in some cases, detection in bone-marrow tissue that predates the transplants. PCR amplification in these samples is dependent on the contribution of the transplanted HSC to blood production, and the sensitivity of each PCR. Gel source data is shown in Supplementary Fig. 1. **c**, List summarizing the rearrangements found in 28 HSC clones and the results from **b**. All 27 rearrangements could be detected by PCR and confirmed by Sanger sequencing. 16/27 (59%) rearrangements could be detected before transplantation.

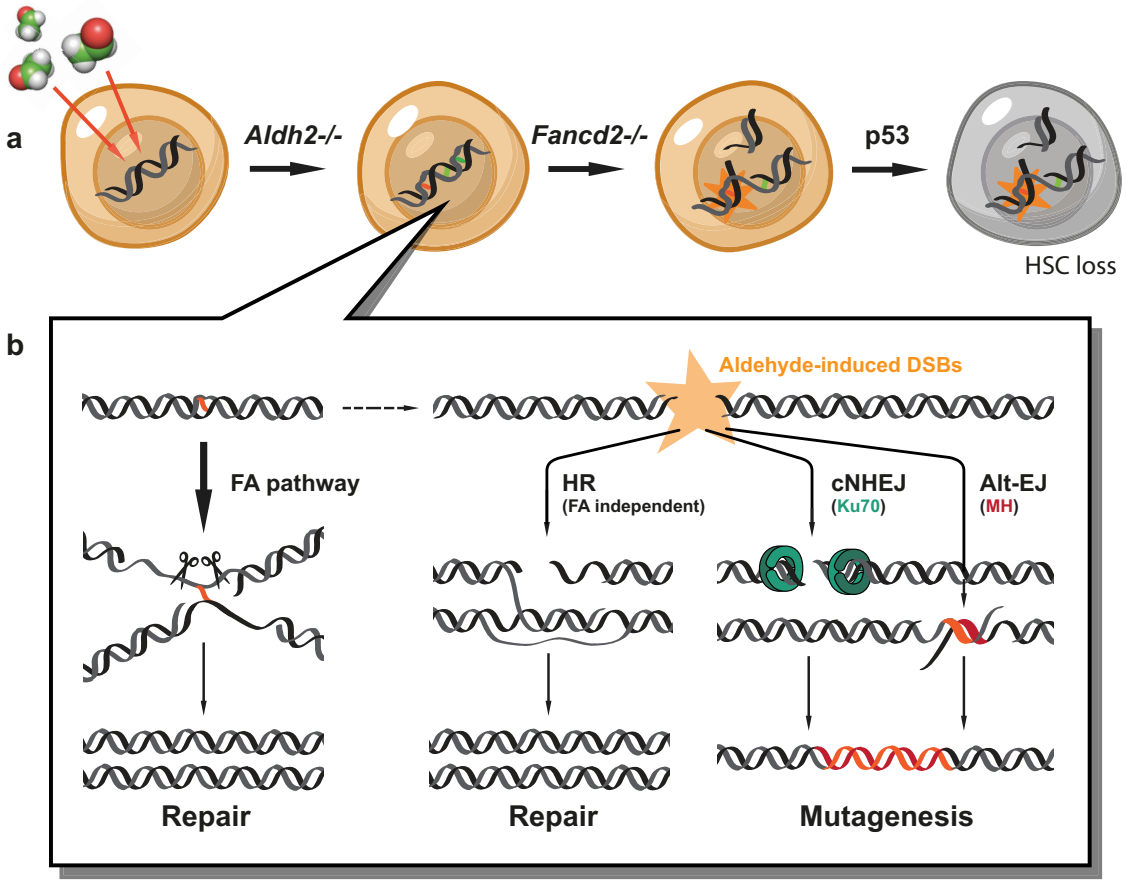

Extended Data Figure 11 | Mechanisms to maintain genetic integrity and suppress mutagenesis by endogenous aldehydes in HSCs. **a**, Aldehyde catabolism and Fanconi anaemia (FA)-pathway-mediated DNA repair constitute two distinct tiers of protection against aldehyde damage. Loss of this protection leads to the accumulation of DNA damage and mutagenesis. Passage of mutated genetic information is prevented by the activation of p53, leading to HSC loss. **b**, In the absence of a functional Fanconi anaemia pathway, aldehyde lesions degenerate into DNA DSBs that can be repaired through error-free recombination. However, this mechanism is not sufficient to fully compensate for Fanconi anaemia inactivation, leading to the engagement of both classical and alternative end-joining, and subsequent mutagenic repair.

nature research

Corresponding author(s): Patel KJ

☐ Initial submission ☐ Revised version ☒ Final submission

Life Sciences Reporting Summary

Nature Research wishes to improve the reproducibility of the work that we publish. This form is intended for publication with all accepted life science papers and provides structure for consistency and transparency in reporting. Every life science submission will use this form; some list items might not apply to an individual manuscript, but all fields must be completed for clarity.

For further information on the points included in this form, see Reporting Life Sciences Research. For further information on Nature Research policies, including our data availability policy, see Authors & Referees and the Editorial Policy Checklist.

Experimental design

1. Sample size

Describe how sample size was determined.

For the analysis of Mendelian segregation of alleles, samples size was determined by power analysis using the following site http://biomath.info/power/chsq1gp.htm. Sufficient animals were used in order to detect a 50% reduction in expected frequency, using power of 0.8 and alpha 0.05. For all other animal experiments, no statistical methods were used to predetermine sample size.

2. Data exclusions

Describe any data exclusions.

No data were excluded from analyses.

3. Replication

Describe whether the experimental findings were reliably reproduced.

All experiments were replicated as stated in the text. All experiments were reproducible on all occasions reproduced.

4. Randomization

Describe how samples/organisms/participants were allocated into experimental groups.

No randomisation was employed

5. Blinding

Describe whether the investigators were blinded to group allocation during data collection and/or analysis.

The investigators were blinded to the genotypes of mice throughout the study and data was acquired relying purely on identification numbers.

Note: all studies involving animals and/or human research participants must disclose whether blinding and randomization were used.

6. Statistical parameters

For all figures and tables that use statistical methods, confirm that the following items are present in relevant figure legends (or in the Methods section if additional space is needed).

n/a	Confirmed
☐	☒ The exact sample size (*n*) for each experimental group/condition, given as a discrete number and unit of measurement (animals, litters, cultures, etc.)
☐	☒ A description of how samples were collected, noting whether measurements were taken from distinct samples or whether the same sample was measured repeatedly
☐	☒ A statement indicating how many times each experiment was replicated
☐	☒ The statistical test(s) used and whether they are one- or two-sided (note: only common tests should be described solely by name; more complex techniques should be described in the Methods section)
☐	☒ A description of any assumptions or corrections, such as an adjustment for multiple comparisons
☐	☒ The test results (e.g. *P* values) given as exact values whenever possible and with confidence intervals noted
☐	☒ A clear description of statistics including central tendency (e.g. median, mean) and variation (e.g. standard deviation, interquartile range)
☐	☒ Clearly defined error bars

See the web collection on statistics for biologists for further resources and guidance.

Software

Policy information about availability of computer code

7. Software

Describe the software used to analyze the data in this study.	Data was analysed using Graphpad prism. NGS data which was analysed with CaVEman, pindel and Brass. Flow cytometry data was analyzed with FlowJo.

For manuscripts utilizing custom algorithms or software that are central to the paper but not yet described in the published literature, software must be made available to editors and reviewers upon request. We strongly encourage code deposition in a community repository (e.g. GitHub). *Nature Methods* guidance for providing algorithms and software for publication provides further information on this topic.

Materials and reagents

Policy information about availability of materials

8. Materials availability

Indicate whether there are restrictions on availability of unique materials or if these materials are only available for distribution by a for-profit company.	All materials are available

9. Antibodies

Describe the antibodies used and how they were validated for use in the system under study (i.e. assay and species).	SCE ASSAY: mouse FITC-conjugated anti-BrdU antibody (Clone B44, BD Biosciences) and goat anti-mouse Alexa fluor-488 secondary antibody (Life Technologies, A-11001). FLOW CYTOMETRY: Micronucleus assay, FITC-CD71 antibody (GenTex, clone R17217.1.4). HSCs FITC-conjugated lineage cocktail with antibodies anti-CD4 (clone H129.19, BD Pharmingen), CD3e (clone 145-2C11, eBioscience), Ly-6G/Gr-1 (clone RB6-8C5, eBioscience), CD11b/Mac-1 (clone M1/70, BD Pharmingen), CD45R/B220 (clone RA3-6B2, BD Pharmingen), Fcε R1α (clone MAR-1, eBioscience), CD8a (clone 53-6.7, BD Pharmingen), CD11c (clone N418, eBioscience), TER-119 (clone Ter119, BD Pharmingen) and anti-CD41 (FITC, clone MWReg30, BD Pharmigen); anti-c-Kit (PerCP-Cy5.5, clone 2B8, eBioscience), anti-Sca-1 (PE-Cy7, clone D7, eBioscience), anti-CD150 (PE, clone TC15-12F12.2, BioLegend) and anti-CD48 (biotin, clone HM48-1, BioLegend). ENGRAFMENT anti-CD4 (FITC, clone H129.19, BD Pharmingen), anti-CD8a (FITC, clone 53-6.7, BD Pharmingen), anti-CD45R/B220 (PerCP-Cy5.5, clone RA3-6B2, BioLegend), anti-CD11b/Mac-1 (PE, clone M1/70, BD Pharmingen), anti-Ly-6G/Gr-1 (PE, clone 1A8, BD Pharmingen), anti-TER-119 (PE-Cy7, clone TER-119, BioLegend), anti-CD45.1 (BV421, clone A20, BioLegend) and anti-CD45.2 (APC, clone 104, BioLegend). MATURE LINEAGES: anti-CD45R/B220 (PE, clone RA3-6B2, BD Pharmingen) and anti-IgM (FITC, clone II/41, BD Pharmingen) for B cell progenitors; anti-TER-119 (FITC, clone TER-119, BD Pharmingen) and anti-CD71 (PE, clone C2, BD Pharmingen) for erythroid maturation; anti-CD11b/Mac-1 (PE, clone M1/70, BD Pharmingen) and anti-Ly-6G/Gr-1 (FITC, clone 1A8, eBioscience) for monocyte/granulocyte progenitors. INTRACELLULAR ANTIGENS: anti-p53 (AlexaFluor647, clone 1C12, Cell Signalling), anti-cleaved caspase-3 (AlexaFluor647, clone D3E9, Cell Signalling). WESTERN BLOT: The FANCA antibody (Cell Signalling, D1L2Z) was used at 1:1000 in 5% w/v BSA, 1X TBS, 0.1% Tween20 at 4°C with gentle shaking, overnight. The anti-VINCULIN (abcam, 129002) was used at 1:4000 in the same conditions. Dako swine anti-rabbit immunoglobulins HRP was used as secondary antibody, at 1:2000 for one hour at room temperature. The antibody was validated with FANCA KO samples.

10. Eukaryotic cell lines

a. State the source of each eukaryotic cell line used.

DT40 cell lines used in this study were described previously. They were generated in our lab (FANCC, FANCC/XRCC2, Nidezwiedz et al., Mol Cell. 2004) or the lab of Shunichi Takeda (HR mutants: Takata, Mol Cell Biol., 2001; Al Abo, Caner Research, 2014).

b. Describe the method of cell line authentication used.

DT40 genetic mutants were validated by southern blot and sensitivity to DNA damaging agents, see above reports for detailed information.

c. Report whether the cell lines were tested for mycoplasma contamination.

All cells lines tested mycoplasma negative

d. If any of the cell lines used are listed in the database of commonly misidentified cell lines maintained by ICLAC, provide a scientific rationale for their use.

N/A

Animals and human research participants

Policy information about studies involving animals; when reporting animal research, follow the ARRIVE guidelines

11. Description of research animals

Provide details on animals and/or animal-derived materials used in the study.

Aldh2-/-Fancd2-/- mice on a C57BL/6 x 129S4S6/Sv F1 background were generated for this study. To this end, the previously reported Fancd2 allele (Fancd2tm1Hou, MGI ID: 2673422, a gift from M. Grompe) was backrossed onto the C57BL/6Jo1a background for ten generations and crossed with Aldh2+/- (C57BL/6N) mice to generate Aldh2+/-Fancd2+/- mice on a pure C57BL/6 background. Likewise, the previously reported Aldh2 allele (Aldh2tm1a(EUCOMM)Wtsi; MGI ID: 4431566, EUCOMM8) was backrossed from C57BL/6N onto 129S6/Sv for five generations and crossed with Fancd2+/- mice to generate Aldh2+/-Fancd2+/- mice on a 129S4S6/Sv background. Finally, Aldh2-/-Fancd2-/- and control mice were generated as F1 hybrids from crosses between Aldh2+/-Fancd2+/- females (129S4S6/Sv, Harwell, UK) and Aldh2+/-Fancd2+/- males (C57BL/6, Harwell UK).

To generate Fanca-/-Ku70-/- mice in a pure C57BL/6 background, Fanca+/-mice (Fancatm1a(EUCOMM)Wtsi; MGI ID: 4434431, C57BL/6N, EUCOMM the generation of which was described in Garaycoechea JI, Nautre 2012) were crossed with Ku70+/-mice (Xrcc6tm1Fwa, MGI ID: 2179954 the generation of which was described in Gu, Y Immunitry 1997), and the Fanca+/-Ku70+/- progeny were then intercrossed to generate all possible genotypes. Pups from these crosses were genotyped at between 2-3 weeks old. For the generation of FancaF/-Ku70-/- Vav1-iCre+ tissue-specific double mutants (also pure C57BL/6), Fanca+/-mice were first crossed with FLP deletor mice (Farley, FW Genesis 2000) to produce the Fanca floxed allele (FancaF or Fancatm1c(EUCOMM)Wtsi). Recombination of the Frt sites was verified by PCR (FL033: GCCTTTGCTGCTCTAATTCCATGT, FL040: TCAGCTCACTGAGACGCAACCTTTT ACACT; and En2A: GCTTCACTGAGTCTCTGGCATCTC) and reconstitution of FANCA expression was verified by western blotting FancaF/F spleen extracts (Figure 3). Fanca+/F mice were then crossed with Ku70+/- mice to eventually produce FancaF/F Ku70+/- mice. Finally, these mice were crossed with Fanca+/-Ku70+/-Vav1-iCre to generate FancaF/-Ku70-/- Vav1-iCre and control mice. The Vav1-iCre allele directs the expression of the iCre recombinase to HSCs and hematopoietic tissues 41, and in this case yields the Fanca null allele (FancaΔ or Fancatm1d(EUCOMM)Wtsi). FancaΔ/Δ mice phenocopy the Fanca-/- mice reported previously, as judged by FANCA expression, sterility and sensitivity to mitomycin C (Figure 3, Extended Data Figure 5).
Similarly to Aldh2-/-Fancd2-/- F1 mice, Aldh2-/-Fancd2-/-p53-/- mice were also generated in a C57BL/6 x 129S4S6/Sv F1 background. Briefly, the p53 allele reported previously 42 was backcrossed onto 129S6/Sv or C57BL/6J for six generations. p53+/- mice were then intercrossed with Aldh2-/-Fancd2+/- mice to establish parental (F0) strains on both genetic backgrounds, which were finally crossed to obtain Aldh2-/-Fancd2-/-p53-/- and control F1 mice.
For single HSC transplantation experiments, we employed CD45.1 homozygous mice on a C57BL/6J x 129S6/Sv F1 background as recipients. CD45.1 (or Ptprca) had been serially backcrossed from B6.SJL onto 129S6/Sv for six generations, with selection at each generation by serotyping with anti-CD45.1 (A20, FITC, BioLegend) and anti-CD45.2 antibodies (104, PE-Cy7, BioLegend).

For the in vivo point mutation assay, mice carrying BigBlue λLIZ shuttle vector repeats (Stratagene) were crossed with Aldh2-/-Fancd2+/- mice on a C57BL/6 x 129S4S6/Sv hybrid background. The resulting mice were inter-crossed to obtain Aldh2-/-Fancd2-/- BigBlue λLIZ and control mice.

All animals were maintained in specific pathogen-free conditions. In individual experiments all mice were matched for gender and age (8-12 weeks).

Policy information about studies involving human research participants

12. Description of human research participants

Describe the covariate-relevant population characteristics of the human research participants.

N/A

nature research

Corresponding author(s): KJ Patel

☐ Initial submission ☐ Revised version ☒ Final submission

Flow Cytometry Reporting Summary

Form fields will expand as needed. Please do not leave fields blank.

Data presentation

For all flow cytometry data, confirm that:

☒ 1. The axis labels state the marker and fluorochrome used (e.g. CD4-FITC).

☒ 2. The axis scales are clearly visible. Include numbers along axes only for bottom left plot of group (a 'group' is an analysis of identical markers).

☒ 3. All plots are contour plots with outliers or pseudocolor plots.

☒ 4. A numerical value for number of cells or percentage (with statistics) is provided.

Methodological details

5. Describe the sample preparation.

Treated or untreated mice (8-12 weeks of age) were bled and 62 µl of blood were mixed with 338 µl of PBS supplemented with 1000 U/mL of heparin (Calbiochem). 360 µl of blood suspension were then added to 3.6 ml of -80°C methanol and placed at -80°C for at least 12 hours. 1 ml of fixed blood cells were then washed with 6 ml of bicarbonate buffer (0.9% NaCl and 5.3 mM NaHCO3). The cells were resuspended in 150 µl of bicarbonate buffer and 20 µl of this suspension was used for subsequent staining. 72 µl of bicarbonbate buffer, 1 µl of FITC-CD71 antibody (GenTex, clone R17217.1.4) and 7 µl of RNaseA (Sigma) were premixed and added to 20 µl of each cell suspension. The cells were stained at 4°C for 45 minutes, followed by addition of 1 ml of bicarbonate buffer and centrifugation. Finally, cells pellets were resuspended in 500 µl of bicarbonate buffer supplemented with 5 µg/ml propidium iodide (Sigma). The samples were analysed immediately on an LSRII analyser (BD) and data analysed with FlowJo 10.0.7

For HSC quantification, bone marrow cells were isolated from tibiae and femurs with staining buffer (PBS supplemented with 2.5 % FCS) and strained through 70 µm meshes. Red cells were lysed by resuspending the cells in 10 ml of red cell lysis buffer (MACS Miltenyi Biotec) for 10 minutes at room temperature. After centrifugation, the cell pellet was resuspended in staining buffer and nucleated cells were counted with 3% acetic acid (StemCell Technologies) on a Vi-Cell XR cell viability counter (Beckman Coulter). 10x106 bone marrow cells were resuspended in 200 µl of staining buffer and stained as described in the methods. The samples were incubated for 15 minutes at 4°C and washed with 2 ml of buffer. The cell pellets were resuspended in 200 µl of staining buffer containing streptavidin-BV421 and incubated for another 15 minutes at 4°C. Finally, cells were washed, resuspended in 500 µl of staining buffer, data acquired on a Fortessa analyser (BD)

To assess the engraftment of single HSCs into irradiated recipients, 50 µl of blood were obtained from the tail vein of recipient mice every two weeks. Red blood cells (RBC) were lysed by the addition of 1 ml of ammonium chloride lysis buffer (155 mM NH4Cl, 10 mM KHCO3, 0.1 mM Na2EDTA, pH 7.2) and incubated for 10 minutes at room temperature. After centrifugation, the cell pellets were resuspended in 100 µl of staining

	buffer and stained with antibodies described in the methods. After the incubation, cells were washed with 3 ml of staining buffer before being resuspended in 250 µl of the same buffer. Samples were run on the Fortessa analyser (BD) with the HTS module.
6. Identify the instrument used for data collection.	LSRII analyser (BD) Fortessa Analyser (BD) iCyt Synergy Sorter (Sony)
7. Describe the software used to collect and analyze the flow cytometry data.	Data was collected using FACSDiva (BD) and processed using FlowJo 10.0.7
8. Describe the abundance of the relevant cell populations within post-sort fractions.	Post sort analysis was not conducted on single cells for HSC transplant. These cells were assessed for their functional ability to engraft and provide long term multi-lineage reconsitution.
9. Describe the gating strategy used.	The gating strategies are outline in the Suppl Figure.

Tick this box to confirm that a figure exemplifying the gating strategy is provided in the Supplementary Information. ☒